RESEARCH ARTICLE

An Orthogonal Learning Bird Swarm Algorithm for Optimal Power Flow Problems

MANZOOR AHMAD[1], **NADEEM JAVAID**[2], **(Senior Member, IEEE)**,
IFTIKHAR AZIM NIAZ[2], **(Senior Member, IEEE), IJAZ AHMED**[3],
AND MUHAMMAD ADNAN HASHMI[4]

[1]Department of Computer Science, COMSATS University Islamabad, Vehari Campus, Vehari 61100, Pakistan
[2]Department of Computer Science, COMSATS University Islamabad, Islamabad 44000, Pakistan
[3]Department of Information Technology, University of Technology and Applied Sciences, Ibri Campus, Ibri 516, Oman
[4]Faculty of Computer Information Science, Higher Colleges of Technology, Abu Dhabi Men's Campus, Abu Dhabi, United Arab Emirates

Corresponding author: Manzoor Ahmad (manzoor_qau@hotmail.com)

ABSTRACT A dominant statistical method, in which the best combination of factors' levels are predicted by analyzing a few representative combinations of factors' levels, named as orthogonal experimental design (OED). The OED is an effective approach for analyzing the effect of multi-levels factors simultaneously and it works on orthogonal learning (OL) strategy. An evolutionary programming based heuristic method has two contradictory features–exploration and exploitation, balancing in these features have significant impact on its optimization performance. We have applied an OED based auxiliary search strategy for enhancing performance of the bird swarm algorithm (BSA) by improving its exploitation search ability. It is a challenging task to keep balance among two contradictory features–exploration and exploitation of a heuristic approach, while addressing optimal power flow (OPF) problems in power systems. In this research study, we have proposed improved BSA (IBSA) for solving the OPF problems in thermal power systems. We have conducted a study of the OPF problems with objective functions-reducing electricity generation cost, emission pollution, and active power loss to measure the efficiency of proposed IBSA. In this work, we have utilized five benchmark functions and solved OPF problems using three IEEE test systems including IEEE-30 bus system, IEEE-57 bus system, and IEEE-118 bus system to verify stability, effectiveness, and performance of proposed IBSA. The statistical and simulation results have indicated that the proposed IBSA has better convergence, efficiency, and robustness features than the original BSA as well as other heuristic approaches. It is observed that lowest electricity generation cost **800.3975**$/h on IEEE-30 bus system, **41663.5500**$/h on IEEE-57 bus system, and **134941.0367**$/h on IEEE-118 bus system have been achieved using proposed IBSA to address the OPF problems. Furthermore, in transmission lines of the power system network minimum active power loss **16.2869**MW has been observed by conducting a case study on the IEEE 118-bus system based on the proposed IBSA approach.

INDEX TERMS Orthogonal learning, bird swarm algorithm, optimal power flow, smart power grid.

I. INTRODUCTION

A. BACKGROUND AND MOTIVATION

In 1962, Carpentier first introduced the optimal power flow (OPF) problem as an extension of the economic dispatch problem in the power system [1]. The OPF problem

The associate editor coordinating the review of this manuscript and approving it for publication was Sergio Consoli.

is a nonlinear, nonconvex, and quadratic nature large-scale optimization problem. Initially, a numerous traditional mathematical approaches [2], [3], [4], [5], [6], [7], [8], [9] are employed to address OPF problems. These mathematical methods include simplified gradient method [2], interior point method [3], mixed integer nonlinear programming (MINLP), [4], nonlinear programming [5], generalized benders decomposition (GBD) [6], newton method [7],

linear programming [8], and linear/quadratic programming [9]. The OPF problem objective function and its imposed constraints are nonlinear in nature and the traditional mathematical methods could not solve it directly due to their linear approach [10]. Due to these limitations of mathematical methods, the OPF problem's nonlinear constraints and objective function are normally transformed into linear form. The conversion from nonlinear to linear form may result in the loss of accuracy and stability of the power system planning and operations.

In the last few decades (since 1980s), numerous meta-heuristic approaches have also been employed to handle OPF problems in networks of power systems. Simulated annealing (SA) [11] and tabu search algorithm (TSA) [12] are single-solution based approaches which focus on improving and modifying a single solution. In literature, various population-based solutions metaheuristic approaches including bird swarm algorithm (BSA) [13], differential evolution (DE) [14], moth swarm algorithm (MSA) [15], differential search algorithm (DSA) [16], and harmony search algorithm (HSA) [17] have also been proposed to address OPF problems.

A metaheuristic approach has two contradictory features – exploration and exploitation, balancing in these features have significant impact on its efficiency and optimization performance. In the exploitation process, a large set of local optima of the problem is evaluated so that a local optimum is found in a local search region. The exploitation also looks away from the current search region, in another dimension of search space for a best local optimal solution. The exploration means finding a global optimum solution to the problem by exploring the search space on a large scale. In the optimization problem, the number of decision variables defines the size of the problem or search space dimension. Intuitively, a large-scale OPF problem's search space in a power system may contain more than one feasible or optimal solution or exponentially enormous local optima. The tuning of decision parameters and finding the most appropriate settings of operating points in the power system is a challenging task. It is also a challenging task to keep balance among two contradictory features – exploration and exploitation of a heuristic approach, while addressing an optimization problem [18]. A better balance in exploration and exploitation may lead to improving search efficiency of a metaheuristic algorithm.

In research literature, various techniques have been proposed for balancing these two features of a metaheuristic algorithm [19], [20], [21]. In study [19], authors have proposed a new search strategy based on crossover and space expanding (SE) strategy – a leader selection to improve optimizing features of the PSO. In this strategy, crossover plays a significant role to keep stability of optimized solutions and enhance convergence by exploiting the problem search space. The SE strategy guides particles to explore the problem's objective search space rapidly. In study [20], authors have introduced a new approach based on exploration

TABLE 1. Abbreviations.

ABC	Artificial bee colony
ACO	Ant colony optimization
BBO	Biogeography based optimization
BTS	Backtracking search
BSA	Bird swarm algorithm
CBO	Colliding bodies optimization
CEFO	Chaotic electromagnetic field optimization
COFS	Constraints-prior object fuzzy sorting
CS	Cuckoo search
DE	Differential evolution
DGWO	Developed grey wolf optimizer
DSA	Differential search algorithm
EA	Evolutionary algorithm
EP	Evolutionary programming
ESA-DE	Enhanced self-adaptive DE
FBA	Firefly-bat algorithm
FBICL	Fuzzy-based improved comprehensive-learning
FI-DE	Forced initialized DE
FOPSO-EE	Fractional order PSO with entropy evolution
GA	Genetic algorithm
GABC	Guided artificial bee colony
GA-MPC	GA based on multi-parent crossover
GBD	Generalized benders decomposition
GBO	Gradient-based optimizer
GSA	Gravitational search algorithm
GSO	Group search optimization
GWSO	Glowworm swarm optimization
HHO	Harris hawk optimization
HSA	Harmony search algorithm
ICA	Imperialist competitive algorithm
ISP-EA	Improved strength pareto EA
IWO	Invasive weed optimization
KHA	Krill herd algorithm
LAPO	Lightning attachment procedure optimization
MBFA	Modified bacteria foraging algorithm
MDE	Modified DE
MFO	Moth flame optimization
MGO	Modified grasshopper optimization
MICA	Modified ICA
MINLP	Mixed integer nonlinear programming
MPA	Marine predator algorithm
MSA	Moth swarm algorithm
MSCA	Modified sine-cosine algorithm
MSFL	Modified shuffle frog leaping
OA	Orthogonal array
OED	Orthogonal experimental design
OL	Orthogonal learning
OPF	Optimal power flow
PPS	Powell's pattern search
PSO	Particle swarm optimization
SA	Simulated annealing
SDP	Semi-definite programming
SHADE	Success history-based adaptive DE
SKH	Stud krill herd
SMA	Slime mould algorithm
SOS	Symbiotic organisms search
SSA	Salp swarm algorithm
SSO	Social spider optimization
TLA	Teaching-learning algorithm
TLBO	Teaching–learning-based optimization
TLSBO	Teaching-learning-studying-based optimizer
TSA	Tabu search algorithm

and exploitation for the PSO to address many objectives of the optimization problem simultaneously more efficiently. The authors named this approach a hybrid global leader

selection (GLS) strategy. A framework based on joint heuristic approaches has been proposed for optimizing the index tracking problem [21]. In literature, these techniques or strategies are broadly classified into: 1) integrating a new search approach into basic heuristic algorithm, 2) heuristic algorithm's variants – adjusting the parameters, 3) neighborhood topologies based enhancement and multi-swarm strategies.

In 1920, R.A. Fisher first introduced a dominant statistical method, orthogonal experimental design (OED) for studying factors' levels combinations. In this method, the best combination of factors' levels has been predicted by analyzing a few representative combinations of factors' levels (experimental test cases) [22]. The OED is an efficient approach for studying the effect of multi-levels factors simultaneously that works on orthogonal learning (OL) strategy. In an optimization problem, the factors are decision or control variables that affect to find feasible value of its objective function. Assigning different values to a factor is considered as levels of a factor. The OED is briefly explained in section III. A wide range of improved metaheuristic approaches also have been designed for efficiently solving OPF problems, in addition to original metaheuristic algorithms. However, an efficient and efficient optimization algorithm is always needed for solving OPF problems.

B. LITERATURE REVIEW

In the last five decades, numerous studies [1], [14], [15], [16], [17], [23], [24], [25], [26], [27], [28], [29], [30], [31], [32], [33], [34], [35], [36] based on original metaheuristic approaches have been documented to find feasible solutions to OPF problems. In these studies different population-based original metaheuristic algorithms including binary backtracking search (BTS) algorithm [1], DE [14], gravitational search algorithm (GSA) [23], glowworm swarm optimization (GWSO) [24], stud krill herd (SKH) [25], tree-seed algorithm [26], biogeography based optimization (BBO) [27], symbiotic organisms search (SOS) [28], semidefinite programming (SDP) [29], salp swarm algorithm (SSA) [30], lightning attachment procedure optimization (LAPO) [31], harris hawk optimization (HHO) [32], multi-objective backtracking search (BTS) algorithm [33], gradient-based optimizer (GBO) [34], slime mould algorithm (SMA) [35], and marine predator algorithm (MPA) [36] have been applied to find feasible solutions of OPF problems.

In Table 1, abbreviations of various methods to find feasible solutions of OPF problems are specified.

Summaries of original algorithms based studies are given in Table 2. In all these studies, OPF problem's objective function - to minimize electricity generation cost (fuel cost) ξ_q based on regular quadratic fuel cost has been studied. In most studies, objectives including minimizing power output cost ξ_{qvp} based on valve-point effect quadratic fuel cost, active power loss P_{loss}, and emission pollution E_p have also been studied. In these studies, one or more IEEE

TABLE 2. Summaries of Studies with Original Algorithms.

Algorithm	Objectives				IEEE Test System		
	ξ_q	ξ_{qvp}	P_{loss}	E_p	30−bus	57−bus	118−bus
BTS [1]	✓	-	-	✓	✓	✓	✓
SA [11]	✓	-	-	-	✓	-	-
TSA [12]	✓	✓	-	-	✓	-	-
DE [14]	✓	✓	✓	✓	✓	✓	✓
MSA [15]	✓	✓	✓	✓	✓	✓	✓
DSA [16]	✓	-	✓	✓	✓	✓	-
HSA [17]	✓	-	✓	-	✓	-	-
GSA [23]	✓	-	✓	✓	✓	-	-
GWSO [24]	✓	-	-	✓	✓	-	-
SKH [25]	✓	✓	✓	✓	✓	✓	-
Tree-Seed [26]	✓	-	✓	-	-	✓	-
BBO [27]	✓	-	-	-	✓	-	-
SOS [28]	✓	✓	-	-	✓	-	-
SDP [29]	✓	-	✓	✓	✓	✓	✓
SSA [30]	✓	-	✓	-	-	✓	✓
LAPO [31]	✓	✓	-	✓	✓	-	-
HHO [32]	✓	-	✓	✓	✓	-	-
BTS [33]	✓	✓	✓	-	-	✓	✓
GBO [34]	✓	✓	✓	✓	✓	✓	✓
SMA [35]	✓	-	✓	✓	✓	✓	✓
MPA [36]	✓	-	✓	-	✓	-	-

test systems have been utilized for evaluating performance of proposed approaches. The standard IEEE-30 bus system has been utilized to evaluate performance of employed heuristic approaches except in studies [26], [30]. The IEEE-57 bus system has been utilized for measuring optimization performance of applied heuristic algorithms in 11 studies. The scalability and optimization performance of heuristic algorithms are tested on the IEEE-118 bus test system in 8 studies.

In literature, it is observed that the majority of heuristic approaches due to scalability issues and the premature convergence property do not perform well to solve the OPF problem in a large-scale power system network such as IEEE-118 bus system. The limitations of some studies are mentioned here. The metaheuristic approach PSO traps in local optima and shows prematurity to find global optimum solution of the optimization problem [23]. In case of addressing large-scale optimization problems, the well-known heuristic approach GA also traps in local optima due to the scalability issue and premature convergence property [37]. The DE has premature and slow convergence characteristics and poorly performs to find a feasible solution of the OPF problem in a large-scale power system [38]. In case of solving the OPF problem in a large-scale power system (i.e. IEEE-118 bus system), the ACO does not find a best feasible solution [39]. In recent literature, numerous improved heuristic and metaheuristic approaches have been documented for finding feasible solutions of OPF problems.

In research literature, to solve OPF problems numerous studies have been conducted by applying various improved

heuristic and metaheuristic approaches such as enhanced ACO (EACO) [39], forced initialized DE (FI-DE) [38], improved strength pareto EA (ISP-EA) [10], improved ABC (IABC) [40], improved CBO (ICBO) [41], AGSO [42], GA-MPC [43], improved GA (IGA) [44], enhanced GA (EGA) [37], modified sine-cosine algorithm (MSCA) [45], FOPSO-EE [46], improved EP (IEP) [47], modified shuffle frog leaping (MSFL) [48], improved PSO (IPSO) [49], improved HSA (IHSA) [50], chaotic self-adaptive differential harmony search (CSA-DHS) [51], Fuzzy HSA [52], multi-Objective EA based decomposition (MOEA/D) [53], efficient EA (EEA) [54], improved BBO (IBBO) [55], developed grey wolf optimizer (DGWO) [56], improved krill herd (IKH) [57], enhanced self-adaptive DE (ESA-DE) [58], modified DE (MDE) [59], cooperative ABC (CABC) [60], modified pigeon-inspired optimization (MPIO) [61], improved SSO (ISSO) [62], improved MFO (IMFO) [63], modified grasshopper optimization (MGO) [64], improved CEFO (ICEFO) [65], and adaptive MFO (AMFO) [66].

Summaries of studies based on improved or enhanced metaheuristic algorithms are available in Table 3. In all studies, the OPF objective – reducing power generation cost ξ_q based on a regular quadratic fuel curve is considered for examining optimization performance of applied approaches. In most studies to evaluate the performance of employed approaches, reducing power generation cost ξ_{qvp} based on a valve-point effect quadratic fuel curve, emission pollution E_p, and active (real) power loss P_{loss} objectives also have been considered. As specified in Table 3, for evaluating scalability and performance of proposed approaches one or more standard IEEE-N bus test systems were utilized. In all these studies, scalability and performance of proposed approaches were measured on the standard IEEE-30 bus system except [59], [66]. In some studies, IEEE-57 bus and IEEE-118 bus test systems were utilized to measure performance and scalability of proposed approaches.

Although numerous research studies based on original and improved or enhanced metaheuristic approaches are conducted for addressing OPF problems. However, an effective and efficient optimization approach to address the large-scale OPF problem is always needed.

C. CONTRIBUTION AND PAPER ORGANIZATION

The bird swarm algorithm (BSA) [67] is a new stochastic swarm intelligence approach. The working model of stochastic bio-inspired BSA based on the birds' social behaviours. The foraging and vigilance behaviours of birds exploit the search space for finding a local optimum. The optimization problem's search space is explored on a global scale by flight behaviour of birds for finding a best feasible solution (global optimum). Due to the stochastic decision for exploiting the optimization problem, the original BSA is trapped in local optima due to premature convergence property [67], [68].

In this research work, we have applied an OED based auxiliary search strategy for enhancing the optimization

TABLE 3. Summaries of studies with improved algorithms.

Algorithm	Objectives				IEEE Test System		
	ξ_q	ξ_{qvp}	P_{loss}	E_p	30−bus	57−bus	118−bus
ISP-EA [10]	✓	-	-	✓	✓	✓	-
EGA [37]	✓	-	✓	-	✓	-	-
FI-DE [38]	✓	-	✓	-	✓	✓	-
EACO [39]	✓	-	-	✓	✓	-	✓
IABC [40]	✓	✓	✓	-	✓	-	✓
ICBO [41]	✓	✓	-	-	✓	✓	✓
AGSO [42]	✓	-	-	✓	✓	✓	-
GA-MPC [43]	✓	✓	-	✓	✓	-	-
IGA [44]	✓	✓	✓	-	✓	-	✓
MSCA [45]	✓	-	✓	-	✓	-	✓
FOPSO-EE [46]	✓	-	✓	-	✓	✓	-
IEP [47]	✓	✓	-	-	✓	-	-
MSFL [48]	✓	-	-	✓	✓	-	-
IPSO [49]	✓	-	✓	✓	✓	-	-
IHSA [50]	✓	✓	-	-	✓	✓	✓
CSA-DHS [51]	✓	✓	-	-	✓	-	-
Fuzzy HSA [52]	✓	-	-	-	✓	✓	✓
MOEA/D [53]	✓	-	✓	✓	✓	✓	-
EEA [54]	✓	✓	-	-	✓	-	✓
IBBO [55]	✓	-	-	-	✓	-	-
DGWO [56]	✓	✓	-	-	✓	-	-
IKH [57]	✓	-	✓	✓	✓	✓	✓
ESA-DE [58]	✓	-	✓	✓	✓	✓	-
MDE [59]	✓	-	✓	-	-	✓	✓
CABC [60]	✓	-	-	-	✓	-	-
MPIO [61]	✓	-	✓	✓	✓	✓	✓
ISSO [62]	✓	✓	✓	✓	✓	-	✓
IMFO [63]	✓	✓	✓	✓	✓	-	✓
MGO [64]	✓	-	✓	✓	✓	✓	✓
ICEFO [65]	✓	-	-	-	✓	-	✓
AMFO [66]	✓	✓	✓	✓	-	-	✓

performance of the BSA by exploiting search ability. We have proposed improved BSA (IBSA) to find feasible solutions to OPF problems. To the best of our knowledge, application of proposed IBSA for solving the OPF problems has not been documented in research literature. This is a main contribution of our research study. The knowledge contributions of our research study are the following:

- We have developed a novel IBSA based on OL strategy by improving the optimization performance of the bio-inspired BSA.
- We have proposed IBSA to find feasible solutions of OPF problems in power systems.

In this study, OPF problem objective functions – reducing electricity generation cost (i.e. regular quadratic fuel cost and valve-point loading effects quadratic fuel cost), emission pollution, and active power loss are studied. We have utilized three transmission networks such as IEEE-30 bus system, IEEE-57 bus system, and IEEE-118 bus system for evaluating and verifying stability, convergence, and optimization performance of the proposed IBSA. We also

have conducted a comparative study with some modern metaheuristic approaches including original BSA, ABC, PSO, DE, and HSA.

The rest of this paper is structured as follows. In section II, the OPF problem and its objective functions are formulated. The details of proposed IBSA approach, original BSA, and OL strategy are described in section III. The brief description of case studies and the details of simulation and statistical results are given in section IV. Finally in the last section V, the conclusion and future work are presented.

II. OPF PROBLEM FORMULATION

The OPF problem is a nonlinear, nonconvex and quadratic nature large-scale optimization problem due to its quadratic nature primary objective function and imposed numerous constraints. Under secure and stable settings of state and control variables aka operating points, a certain objective has been achieved in solving the OPF problem. Its mathematical formulation can be described as [14]:

$$
\begin{aligned}
Minimize: \quad & f(x, u) \\
subject\, to: \quad & g(x, u) = 0 \\
& h(x, u) \leq 0
\end{aligned}
\tag{1}
$$

where, function $f(x, u)$ represents the OPF problem objective, x is a set of state or dependent variables that describes the state of the power system network and u is a set of control variables that controls the power flow in a power system. The term $g(x, u)$ represents equality constraints and $h(x, u)$ represents inequality constraints. All these constraints must be satisfied in solving the OPF problem. Further details of variables and constraints are given in sub-sections.

A. CONTROL OR INDEPENDENT VARIABLES

Control or independent variables play a significant role to control the power flow in a power system. Active or real power P_G output from thermal energy sources excluding at swing bus, voltage magnitude V_G of energy sources, shunt capacitors Q_C on selected buses, and transformers tap T settings on selected branches are considered as control variables. In the form of vector u, control variables can be defined as [14]:

$$
u = \left[P_{G_i} \dots P_{G_{NG}}, V_{G_i} \dots V_{G_{NG}}, Q_{C_j} \dots Q_{C_{NC}}, T_k \dots T_{NT} \right]
\tag{2}
$$

where P_{G_i} represents active power generation from the energy source at bus $i \in [1, 2, \dots, NG]$ except the energy source at the swing bus and NG is the number of energy sources. The term V_{G_i} is voltage magnitude of generator at i^{th} bus, Q_{C_j} represents shunt capacitor at j^{th} bus, and T_k represents transformer tap at branch k. The term NC is shunt capacitors, and NT represents the number of transformers tap.

B. STATE OR DEPENDENT VARIABLES

There is a need for dependent variables for describing the state of a power system network. Active (real) power P_G of

the swing bus energy source, reactive power Q_G of all energy sources, all load buses voltage magnitude V_L, and line load S_L of transmission lines are dependent or state variables. In the form of vector x, state or dependent variables can be written as [14]:

$$
x = \left[P_{G_i}, V_{L_p} \dots V_{L_{NL}}, Q_{G_i} \dots Q_{G_{NG}}, S_{L_q} \dots S_{L_{Nl}} \right]
\tag{3}
$$

where P_{G_i} is the active (real) power output of an energy source at swing i^{th} bus. The term V_{L_p} is the voltage magnitude of PQ or load buses, $p = [1, 2, \dots, NL]$, and the term NL represents PQ or load buses. The term Q_{G_i} is reactive power produced from an energy source at i^{th} bus, S_{L_q} is line loading of transmission line q, and Nl represents transmission lines.

C. CONSTRAINTS

In the OPF problem, finding the best fitness value of objective is subject to satisfying equality and inequality constraints. Active (real) power flow and reactive power flow equations are named as equality constraints. Security constraints on transmission lines, operating limits of equipment, and voltage magnitude limits on load buses are named as inequality constraints and their details are given below.

1) EQUALITY CONSTRAINTS

The active power P_{Gi} output from the thermal energy source attached at bus i^{th} should be equal to the sum of active (real) power (i.e. load demand) and active power loss, $\forall i \in NB$ (number of buses). Similarly, reactive power Q_{Gi} output from the thermal energy source attached at bus i^{th} would be required to equal reactive power demand and reactive power loss, $\forall i \in NB$. The mathematically equality constraints can be written as [14]:

$$
P_{Gi} = P_{Di} + V_i \sum_{j=1}^{NB} V_j \{ G_{ij} cos(\theta_{ij}) + B_{ij} sin(\theta_{ij}) \} \quad \forall i \in NB
\tag{4}
$$

$$
Q_{Gi} = Q_{Di} + V_i \sum_{j=1}^{NB} V_j \{ G_{ij} sin(\theta_{ij}) - B_{ij} cos(\theta_{ij}) \} \quad \forall i \in NB
\tag{5}
$$

where the terms P_{Gi} and Q_{Gi} represent active and reactive power generation from an energy source connected at i^{th} bus. The terms P_{Di} and Q_{Di} are active and reactive load demand at i^{th} bus. The terms V_i and V_j are voltage magnitude at i^{th} bus and j^{th} bus. The term $\theta_{ij} = \theta_i - \theta_j$ is voltage angle difference. The term B_{ij} represents transfer susceptance and G_{ij} is conductance between i^{th} bus and j^{th} bus.

2) INEQUALITY CONSTRAINTS

In power systems, stable and secure physical settings of equipment and operational boundary limits are reflected by inequality constraints. The operating limits of generators, shunt capacitors, transformers tap settings, security constraints on transmission lines, and voltage magnitude limits of load buses are referred to as inequality constraints. These

constraints ensure security of power system and categorized as follows:

a: GENERATORS' CONSTRAINTS

$$P_{Gi}^{min} \leq P_{Gi} \leq P_{Gi}^{max} \quad \forall i \in NG \qquad (6)$$

$$Q_{Gi}^{min} \leq Q_{Gi} \leq Q_{Gi}^{max} \quad \forall i \in NG \qquad (7)$$

$$V_{Gi}^{min} \leq V_{Gi} \leq V_{Gi}^{max} \quad \forall i \in NG \qquad (8)$$

where superscripts "min" and "max" are boundary limits of P_{Gi}, Q_{Gi}, and V_{Gi} variables.

b: SHUNT CAPACITOR (COMPENSATOR) CONSTRAINTS

$$Q_{C_j}^{min} \leq Q_{C_j} \leq Q_{C_j}^{max} \quad \forall j \in NC \qquad (9)$$

where term Q_{C_j} is volt-ampere reactive (VAR) injected by j^{th} shunt capacitor (compensator) and $Q_{C_j}^{min}$ and $Q_{C_j}^{max}$ are boundary limits of jth shunt compensator. NC represents the total number of the shunt compensators.

c: TRANSFORMER TAP CONSTRAINTS

$$T_k^{min} \leq T_k \leq T_k^{max} \quad \forall k \in NT \qquad (10)$$

where T_k indicates transformer tap setting located at bus k and T_k^{min} and T_k^{max} are boundary limits. NT represents the total number of transformers.

d: SECURITY CONSTRAINTS

$$V_{L_p}^{min} \leq V_{L_p} \leq V_{L_p}^{max} \quad \forall p \in NL \qquad (11)$$

$$S_{L_q} \leq S_{L_q}^{max} \quad \forall q \in N_l \qquad (12)$$

where V_{L_p} represents voltage magnitude on load bus p and terms $V_{L_p}^{min}$ and $V_{L_p}^{max}$ are boundary limits imposed on voltage magnitude. The term NL shows the total number of PQ or load buses. The term S_{L_q} represents line flow of transmission line q and $S_{L_q}^{max}$ is maximum line flow on q transmission line. N_l represents transmission lines.

D. OBJECTIVE FUNCTIONS

We have conducted a study on OPF problems with four objective functions in thermal energy-based small-scale to large-scale power systems. Generating electrical power using fossil fuels like coal, oil, and natural gas in thermal generators are primary sources of harmful gases or green gases emission into the atmosphere. The electricity generation cost of a thermal energy source can be formulated as a regular quadratic cost curve and its three different forms; 1) piecewise quadratic cost curve, 2) prohibited operating zones quadratic cost curve, and 3) valve-point loading effect quadratic cost curve. We have made an assumption in this research work that the same fuel is used in all thermal energy sources for electricity generation. We have applied the proposed IBSA to solve OPF problems, considering four objectives:

1) Minimizing electricity generation cost based on regular quadratic fuel cost).

2) Minimizing electricity generation cost based on valve-point loading effects quadratic fuel cost.
3) Minimizing active power loss in transmission lines of power system.
4) Minimizing carbon emission pollution into the atmosphere due to burn of fossil fuels in thermal power plants.

1) QUADRATIC FUEL COST
In a thermal energy-based power system, fossil fuel cost ($/h) has a quadratic relationship with power output (MW) from energy source (i.e. generator) [14]:

$$f_1(x, u) = \sum_{i=1}^{NG} a_i + b_i P_{G_i} + c_i P_{G_i}^2 \qquad (13)$$

where terms a_i, b_i, and c_i represent cost coefficients and term P_{G_i} is active power generation from thermal energy source (generator) connected at i^{th} bus.

2) VALVE-POINT LOADING EFFECTS QUADRATIC FUEL COST
A steam turbine has multi-valve that exhibit a large variation in fossil fuel consumption in the thermal generator. Therefore, in this study for realistic and precise modeling of power generation cost of thermal power plants, we have included valve-point loading effects in calculating fuel cost. It can be formulated as a sinusoidal function to measure fuel cost [14]:

$$f_2(x, u) = \sum_{i=1}^{NG} a_i + b_i P_{G_i} + c_i P_{G_i}^2$$
$$+ \left| d_i \times sin\left(e_i \times (P_{G_i}^{min} - P_{G_i})\right) \right| \qquad (14)$$

where terms a_i, b_i, and c_i represent fossil fuel cost coefficients and terms d_i and e_i are cost coefficients based on valve-point loading effects of energy source connected at i^{th} bus. $P_{G_i}^{min}$ indicates the minimum active power generation capacity of an energy source at i^{th} bus. P_{Gi} is active (real) power output from a thermal energy source connected at i^{th} bus.

3) ACTIVE POWER LOSS
The active (real) power loss is unavoidable in a power system because of inherent reactance and resistance in transmission lines. Reducing active power loss has significant effects on operations and planning of the power system and control or independent variables are also optimized for this purpose. The mathematically active power loss (MW) is written as [14]:

$$f_3(x, u) = \sum_{q=1}^{Nl} G_{q(ij)} \left\{ V_i^2 + V_j^2 - 2V_i V_j cos(\theta_{ij}) \right\} \qquad (15)$$

where term Nl indicates number of transmission lines and term $G_{q(ij)}$ represents transfer conductance of transmission line q connecting i^{th} bus and j^{th} bus. The terms V_i and V_j represent voltage magnitude at i^{th} and j^{th} buses. The term $\theta_{ij} = \theta_i - \theta_j$, is voltage angle difference among i^{th} bus and j^{th} bus.

4) EMISSION POLLUTION

It is well known that primary source of harmful gases such as carbon monoxide (CO), NO_x, CO_x, and SO_x emission into the atmosphere is burning of fossil fuels in thermal power plants. It has become necessary with climate changes and global environmental concerns, to regulate thermal energy based power systems by reducing emission pollution. The harmful gases emission (ton/h) into atmosphere during power generation from thermal energy source has been measured as follows [14]:

$$f_4(x, u) = \sum_{i=1}^{NG} \left\{ (\alpha_i + \beta_i P_{G_i} + \gamma_i P_{G_i}^2) \times 0.01 + \omega_i e^{(\mu_i P_{G_i})} \right\}$$
(16)

where terms α_i, β_i, γ_i, ω_i, and μ_i represent emission coefficient for energy source connected at i^{th} bus.

III. ORTHOGONAL LEARNING BIRD SWARM ALGORITHM

In addition to the traditional mathematical methods, numerous nature-inspired and bio-inspired metaheuristic approaches have been proposed for solving optimization problems in research literature [23], [24], [25], [26], [27], [28], [29], [30], [31], [32], [33], [34], [35], [36]. The bird swarm algorithm (BSA) [67] is a new population-based stochastic swarm intelligence approach. The original BSA has premature convergence and poor capability to escape from local optima due to the stochastic decision for exploitation of search space of high dimensional optimization problems [67], [68]. We have applied an OED based auxiliary search strategy to enhance optimizing features of the BSA by efficiently exploiting local regions of search space in this research work. We have proposed the improved BSA (IBSA) for solving OPF problems.

A. ORIGINAL BIRD SWARM ALGORITHM

In the BSA [67], swarm intelligence, based on birds' social behaviours, has been employed for solving the optimization problem. In BSA, four search approaches including vigilance, foraging, scrounger, and producer are efficiently regulated to explore and exploit the optimization problem search space. A bird's interactions in swarm and social behaviours can be easily understood based on following five well-defined rules:

1) In this rule, a stochastic decision based on bird's foraging behaviour probability P. Every bird in the swarm may have foraging behaviour or vigilance behaviour. If probability P is greater than the stochastically selected value from $rand(0, 1)$, the bird swaps into foraging behaviour, otherwise the bird has vigilance behaviour.

2) In this rule, every bird in a swarm updates its fitness to search for food items based on social behaviour and the swarm's best experience. This information such as the swarm's best experience and bird's social behaviour are shared in the bird's swarm immediately. It can be

mathematically modeled as [67]:

$$x_{i,j}^{t+1} = x_{i,j}^t + (p_{i,j} - x_{i,j}^t) \times \delta \times rand(0, 1) + (g_j - x_{i,j}^t) \times \tau \times rand(0, 1)$$
(17)

where $i \in \{1, 2, \ldots, N\}$ indicates i^{th} bird in N birds and $j \in \{1, 2, \ldots, D\}$ represents the jth dimension of D dimensions of optimization problem search space. The term $x_{i,j}^t$ represents the ith bird's position in the jth dimension of search space for possible flight of birds at time t and these birds may have foraging or vigilance behaviour. δ is cognitive accelerated positive coefficient and τ is social accelerated positive coefficient. The term $p_{i,j}$ represents the previous best position of the ith bird in the swarm. The term g_j represents the best previous position (global optimal) shared by the swarm. The term $rand(0, 1)$ is a function of uniform distribution.

3) Every bird in the swarm wishes to move in the direction of the swarm's center due to its vigilance behaviour. This movement of each bird towards the center of the swarm may be affected by competition among birds to reach the swarm's center. According to this rule, birds could not move in the direction of the swarm's center directly. The vigilance behaviour of bird can be modeled as [67]:

$$x_{i,j}^{t+1} = x_{i,j}^t + \Upsilon_1 (mean_j - x_{i,j}^t) \times rand(0, 1) + \Upsilon_2 (p_{k,j} - x_{i,j}^t) \times rand(-1, 1)$$
(18)

$$\Upsilon_1 = \upsilon_1 \times exp\left(- \frac{pFit_i}{sumFit + \varepsilon} \times N \right)$$
(19)

$$\Upsilon_2 = \upsilon_2 \times exp\left\{ \left(\frac{pFit_i - pFit_k}{|pFit_k - pFit_i| + \varepsilon} \right) \frac{N \times pFit_k}{sumFit + \varepsilon} \right\}$$
(20)

where term $mean_j$ is the jth bird mean position in the swarm. $k \in \{1, 2, \ldots, N\}$ and $k(k \neq i)$ is a randomly selected positive integer. The terms υ_1 and υ_2 represent two positive constants within range [0,2]. The term $pFit_i$ indicates i^{th} bird's best fitness value. The term $sumFit$ indicates swarm total fitness value (or sum of each bird's best fitness in the swarm). ε represents the very small positive constant to prevent the error of zero division.

Every bird in the swarm moves towards the center of the swarm due to direct and indirect effects. The force induced by birds' social behaviours and environments affects the swarm's mean fitness and it is calculated as an indirect effect. Other force induced by specific interference is calculated as direct effect and Υ_2 is applied for simulating it. The scenario $\Upsilon_2 > \upsilon_2$ occurs, if $k^{th}(k \neq i)$ bird has a better fitness value than i^{th} bird. It means the kth bird may suffer from a smaller interference force than the ith bird. On the basis of unpredictability and some randomness, k^{th} bird would be more likely to travel in the direction of the swarm's

TABLE 4. Experimental design for chemical reaction.

Levels	Factors		
	A:Temperature(^{o}C)	B:Oxygen (cm^3)	C:Water(%)
L_1	80	90	5
L_2	85	120	6
L_3	90	150	7

center than i^{th} bird. The minimum fitness value of a bird in a swarm defines the global optimum or best feasible value for solving the minimal optimization problem.

4) In the swarm, birds switch to flight behaviour by flying from one site to another site in any direction and this flight behaviour may be due to birds' foraging behaviour, predation threat or any other circumstances. After arriving on a new site, birds often swapped into two groups of birds such as scrounger and producer during foraging for food patches. The birds' behaviours including producer and scrounger mathematically can be formulated as [67]:

$$x_{i,j}^{t+1} = x_{i,j}^t + randn(0, 1) \times x_{i,j}^t \quad (21)$$

$$x_{i,j}^{t+1} = x_{i,j}^t + \left(x_{k,j}^t - x_{i,j}^t\right) \times FL \times rand(0, 1) \quad (22)$$

where, $k \in \{1, 2, \ldots, N\}$ and $k(k \neq i)$, indicates a positive integer. $FL(FL \in \{0, 2\})$ means that for searching food patches, the producer would be followed by scrounger.

5) After arriving on a new site, food patches are explored actively by producers and scroungers randomly follow producers for searching food patches.

B. ORTHOGONAL EXPERIMENTAL DESIGN

In order to present the concept of OED method and how to use it, a simple example is considered based on a chemical reaction experiment [69]. In this chemical reaction experiment, the chemical conversion rate depends on three quantities such as temperature (^{o}C), amount of oxygen (cm^3), and water percentage (%), which are respectively interpreted as A, B, and C factors of the experiment. In Table 4, there are three different values of each factor denoted as levels L1, L2, and L3. For example, the amount of oxygen can be 90, 120, or 150 cm^3. In this example, a total $3^3 = 27$ combinations of factors' levels are possible and so 27 experimental test cases have been derived for finding the best chemical conversion rate. In general, the possible combinations of factors' levels can be calculated as Q^N, where N represents factors and Q represents levels per factor. It may be impractical to conduct a large number of experimental test cases Q^N to find the best combination of levels for chemical conversion rate when Q and N are very large. In such a case to reduce experimental testing cost, it is required to use small representative combinations of factor's levels instead of all combinations of factor's levels. The OED plays a significant role in predicting a small set of representative combinations based on "fractional factorial" experiments. For a better

TABLE 5. Best combinations using OED and factors analysis.

Combination	A:Temperature (^{o}C)	B:Oxygen (cm^3)	C:Water (%)	Results
C_1	(1) 80	(1) 90	(1) 5	$f_1 = 31$
C_2	(1) 80	(2) 120	(2) 6	$f_2 = 54$
C_3	(1) 80	(3) 150	(3) 7	$f_3 = 38$
C_4	(2) 85	(1) 90	(2) 6	$f_4 = 53$
C_5	(2) 85	(2) 120	(3) 7	$f_5 = 49$
C_6	(2) 85	(3) 150	(1) 5	$f_6 = 42$
C_7	(3) 90	(1) 90	(3) 7	$f_7 = 57$
C_8	(3) 90	(2) 120	(1) 5	$f_8 = 62$
C_9	(3) 90	(3) 150	(2) 6	$f_9 = 64$
Factors Analysis				
Levels	A:Temperature(^{o}C)	B:Oxygen (cm^3)	C:Water(%)	
L_1	$H_{A1} = (f_1+f_2+f_3)/3 = 41$	$H_{B1} = (f_1+f_4+f_7)/3 = 47$	$H_{C1} = (f_1+f_6+f_8)/3 = 45$	
L_2	$H_{A2} = (f_4+f_5+f_6)/3 = 48$	$H_{B2} = (f_2+f_5+f_8)/3 = 55$	$H_{C2} = (f_2+f_4+f_9)/3 = 57$	
L_3	$H_{A3} = (f_7+f_8+f_9)/3 = 61$	$H_{B3} = (f_3+f_6+f_9)/3 = 48$	$H_{C3} = (f_3+f_5+f_7)/3 = 48$	
Best	A3	B2	C2	

understanding of the OL strategy, the important terms are described herein.

1) ORTHOGONAL ARRAY

The array is termed as orthogonal because all factors in an orthogonal array (OA) can be independently evaluated. In which the core effect of one multi-levels factor on response variables (results or objectives) does not influence to measure the effect of another multi-levels factor. By OA, nominated combinations of factors' levels are uniformly distributed over the all possible combinations of levels which guarantees a secure and stable comparison of individual factor's levels. In OA, an individual row indicates the factors' levels in every combination, while an individual column indicates a particular factor that may be altered from every combination.

Let's consider N factors and each factor consists of three different levels. For a complete experiment, a total 3^N number of experimental test cases or combinations of levels are required. The notation $L_M(Q^N)$ is used to represent an array for N factors with Q levels of each factor, where L represents an array and M represents number of rows and each row is a combination of levels. In such case to construct an $OA = L_M(3^N)$ with M rows for N factors, an integer $M = 3^{\lceil \rceil^{log_3(2N+1)}}$, where $\lceil \rceil$ is a ceiling function. Based on a chemical reaction experiment specified in Table 4, an array is defined that contains 9 representative combinations of levels for 3 factors in which each factor has 3 levels, as follows:

$$L_9(3^3) = \begin{bmatrix} 1 & 1 & 1 \\ 1 & 2 & 2 \\ 1 & 3 & 3 \\ 2 & 1 & 2 \\ 2 & 2 & 3 \\ 2 & 3 & 1 \\ 3 & 1 & 3 \\ 3 & 2 & 1 \\ 3 & 3 & 2 \end{bmatrix} \quad (23)$$

An array $[a_{i,j}]_{M \times N}$ has index t and strength λ on $0 \leq \lambda \leq Q$ is defined as OA when every sub-array $[a_{i,j}]_{M \times \lambda}$ of A consists of all representative combinations of ordered $\lambda - tuple$ exactly

t times as a row. An example of $[a_{i,j}]_{9\times 3}$ OA which has index $t = 1$ and strength $\lambda = 2$ specified in Eq. 23. It consists of ordered 2-tuples or ordered pairs (1, 1), (1, 2), (1, 3), (2, 1), (2, 2), (2, 3), (3, 1), (3, 2), and (3, 3) that occur only one time in any two columns. As stated above, few experimental test cases are conducted based on OED for finding the best representative combination of levels. Based on OED, the total nine experimental test cases identified by $L_9(3^3)$ are specified in Table 5. For example, the first representative experimental test case is first combination of levels (C_1) and represents the first row [1 1 1] in OA. In this experimental test case, factor A (temperature ^oC), factor B (amount of oxygen cm^3), and factor C (water percentage) have been designed to the initial level of each factor such as 80 ^oC, 90 cm^3, and 5%, respectively. Similarly, the second experimental test case is the second combination of levels (C_2) and represents the second row [1 2 2] in OA, and so on.

2) FACTOR ANALYSIS

A systematic technique to find the best factors' levels combination for evaluating the influence of every factor's levels on experimental outcomes is named as factor analysis. It has been conducted on experimental outcomes of all known M test cases of OA for finding the best factors' levels combination. This process is explained herein.

Let f_m is the response variable or experimental test case result of mth combination of levels, where $1 \leq m \leq M$. The H_{nq} represents the average effect of the qth level of the nth factor, where $1 \leq q \leq Q$ and $1 \leq n \leq N$. The average effect H_{nq} for a chemical reaction experiment is calculated as follows [70]:

$$H_{nq} = \frac{\sum_{m=1}^{9} f_m \times Z_{mnq}}{\sum_{m=1}^{9} Z_{mnq}} \quad (24)$$

where $Z_{mnq} = 1$, if the mth combination ($m = 1, 2, 3, \ldots, 9$) is with the qth level ($q = 1, 2, 3$) of the nth factor ($n = A, B, C$), otherwise $Z_{mnq} = 0$.

For instance, measured effect of L_1 on factor A (temperature ^oC), represented by A1. By inspecting 2nd column of Table 4, we observe that combinations of levels C_1, C_2 and C_3 contain all the experimental test cases of L_1 for factor A. The corresponding combination results are $f_1 = 31$, $f_2 = 54$ and $f_3 = 38$ and the mean effect is $H_{A1} = 41$. After measuring mean effects H_{nq} of all levels for every factor, the best combination of factor's levels of every factor can be obtained by choosing H_{nq} with higher value for each factor in case of maximization problem. The factor analysis base results for a chemical reaction experiment are specified in Table 5 and the details of factor analysis are explained in [69]. From Table 5, the best combination of factors' levels for a chemical reaction experiment discovered by factor analysis is A3, B2 and C2. Although this combination temperature 90^oC, amount of oxygen $120cm^3$, and water 6% is not
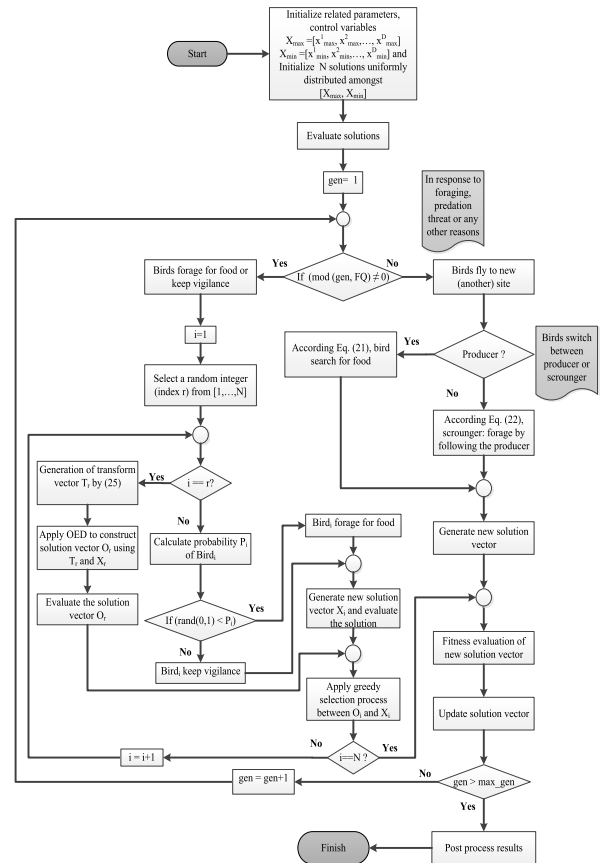
FIGURE 1. Improved BSA working model.

included in the nine experimental test cases (combinations of levels). We have implemented OL strategy in order to improve BSA optimization performance for finding optimal solutions efficiently based on OED.

C. ORTHOGONAL LEARNING BIRD SWARM ALGORITHM

An evolutionary programming based heuristic method has two contradictory features such as exploration and exploitation, balancing in these features have significant impact on its search efficiency and optimization performance. As mentioned before, the original BSA has premature convergence and poor capability to avoid trap into local optima due to a stochastic decision for exploitation of the search space of high dimensional optimization problems. Therefore, we have proposed OL strategy to enhance optimization performance of original BSA by improving the ability of exploitation of search space dimensions. The number of decision or control variables are referred to as a search space dimension or a solution vector dimension. For instance, if the optimization problem contains 10 control variables, it is interpreted as a 10-dimensional search space optimization problem.

In IBSA, optimization process starts by initializing parameters, control variables $X_{max} = [x^1_{max}, x^2_{max}, \ldots, x^D_{max}]$, $X_{min} = [x^1_{min}, x^2_{min}, \ldots, x^D_{min}]$ and N solutions uniformly distributed amongst $[X_{max}, X_{min}]$. The fitness of the initial solution vector is evaluated in the next step, before exploring

TABLE 6. Benchmark functions.

Name	Formula	Dimensions (d)	Search domain	Global optimum
Ackley	$f(x) = -a\exp\left(-b\sqrt{\frac{1}{d}\sum_{i=1}^{d}x_i^2}\right) - \exp\left(\frac{1}{d}\sum_{i=1}^{d}\cos(c\,x_i)\right) + a + \exp(1)$	200	$x_i \in [-32.768, 32.768]$	0
Griewank	$f(x) = \sum_{i=1}^{d}\frac{x_i^2}{4000} - \prod_{i=1}^{d}\cos(\frac{x_i}{\sqrt{i}}) + 1$	200	$x_i \in [-600, 600]$	0
Rastrigin	$f(x) = 10d + \sum_{i=1}^{d}\left(x_i^2 - 10\cos(2\pi x_i)\right)$	200	$x_i \in [-5.12, 5.12]$	0
Rosenbrock	$f(x) = \sum_{i=1}^{d-1}\left[100(x_{i+1} - x_i^2)^2 + (x_i - 1)^2\right]$	200	$x_i \in [-2.048, 2.048]$	0
Sphere	$f(x) = \sum_{i=1}^{d}x_i^2$	200	$x_i \in [-5.12, 5.12]$	0

and exploiting search space. Procedure of searching optimal solution switched into exploring or exploiting search space based on birds' flight behaviours frequency FQ. The foraging and vigilance behaviours of birds exploit the search space for finding a local optimum and flight behaviour of birds explores the search space to find global optimum solution. During exploration of the search space, birds often swapped into two groups of birds such as scrounger and producer during foraging for food patches based on their food reserves.

The procedure of applying OL strategy to determine best exploitation of original BSA is explained onward. Initially, a random integer (index) r is selected. In next step whenever the current candidate solution index i is not equal to randomly selected index r ($i \neq r$), a stochastic decision based on bird's foraging behaviour probability P. Every bird in the swarm may have foraging behaviour or vigilance behaviour. If the stochastically selected value from $rand(0, 1)$ is greater than probability P, the bird swaps into vigilance behaviour, otherwise the bird has foraging behaviour. In other case, whenever the current candidate solution index i is equal to randomly selected index r ($i == r$), a new transmission solution vector T_r mathematically formed as:

$$T_r = X_j + rand(0, 1) \times (X_{best} - X_j), \quad j \neq r \in [1, N] \tag{25}$$

where X_{best} represents an optimal solution based on best fitness value in current iteration, X_j represents the jth solution of N optimal solutions which is not the same as current solution X_r.

In the current iteration, the OL strategy is applied for predicting an optimal solution vector O_r by merging transmission solution vector T_r and current solution vector X_r with few experimental test cases based on OED. To reduce computational cost, OL strategy is used once at each iteration when randomly selected index r is equal to current index i ($i == r$). The detailed working model (flowchart) of the IBSA is shown in Figure 1.

The goal of utilizing OL strategy is to obtain an optimal solution. In this strategy the OED has been applied to conduct few experimental test cases instead of exhaustive

experimental test cases for predicting the best combination of every dimension of two candidate solution vectors. The process to obtain a solution vector O_r by OL strategy is described as following steps:

1) Construct a two-level OA $L_M(2^D)$ of D factors, with $M = 2^{\lceil\rceil\,log_2(D+1)}$, where M represents number of combinations or rows in OA, D is the number of columns in OA or dimension of problem and $\lceil\rceil$ is a ceiling function. The reason behind constructing two-level OA is that in our case, there are two solution vectors such as transmission solution vector T_r and current solution vector X_r used for OL strategy. A procedure for constructing a two-level OA for D factors is written as follows [69]:

```
1:  procedure Generate_OA(OA, D)
2:      M := 2^⌈⌉log₂(D+1);
3:      for i := 1 : M do
4:          for j := 1 : D do
5:              level := 0;
6:              k := j;
7:              mask := M/2;
8:              while k > 0 do
9:                  BAnd := bitwiseAnd(i − 1, mask);
10:                     ▷ // where mask = 2^(m−1) and
11:                     ▷ // bitwiseAnd(α, mask)
12:                 ▷ // returns mᵗʰ least significant bit of α
13:                 if (k mod 2) & (BAnd ≠ 0) then
14:                     level := (level + 1) mod 2;
15:                 endif
16:                 k := ⌊k/2⌋;
17:                 mask := mask/2;
18:                 OA[i][j] := level + 1;
19:             endwhile
20:         endfor
21:     endfor
22: endprocedure
```
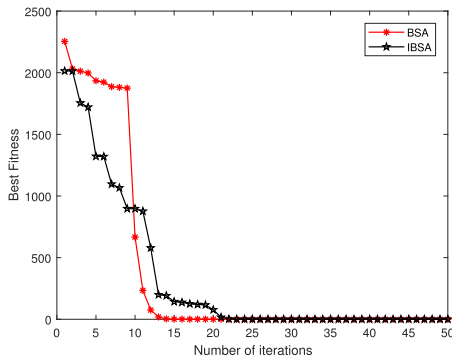
2) The two-level OA $L_M(2^D)$ for D factors (control variables of problem) is filled by choosing '1' for the values of transmission vector T_r and '2' for the values of current solution vector X_r.
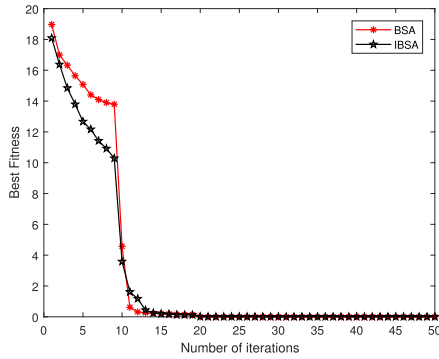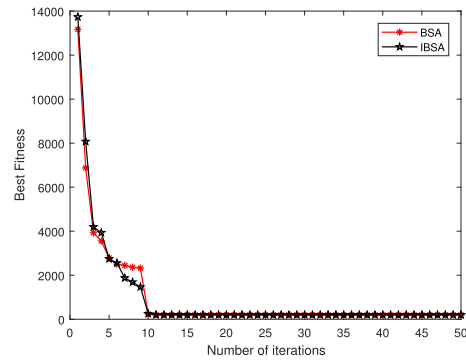
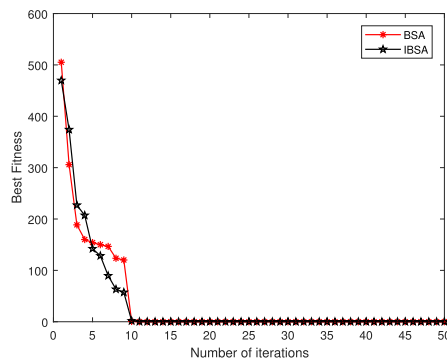(a) Algorithms' convergence properties on *Ackley*
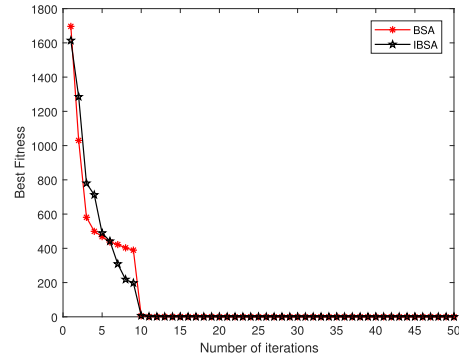
(b) Algorithms' convergence properties on *Griewank*

(c) Algorithms' convergence properties on *Rastrigin*

(d) Algorithms' convergence properties on *Rosenbrock*

(e) Algorithms' convergence properties on *Sphere*

FIGURE 2. Algorithms' convergence properties on benchmark functions.

3) Obtain M experimental test results $f_m (1 \leq m \leq M)$ based on corresponding value of transmission vector T_r (25) and current solution vector X_r according to a two-level OA $L_M (2^D)$ for D factors.

4) Using factor analysis each experimental test result $f_m (1 \leq m \leq M)$ is evaluated based on fitness value and the average effect of experimental results (combination of factors' levels) H_b is measured according to (24).

5) Using factor analysis the best combination of levels for every factor (control variable) is obtained. Based on these best levels, the best combination of factors'

levels H_p is predicted and H_p is evaluated with fitness values.

6) If H_p has the best fitness value as compared to H_b, it is selected as solution vector O_r.

IV. SIMULATION RESULTS AND CASE STUDIES

In this section, we have evaluated the optimization performance and efficiency of proposed IBSA, in order to verify the effect of the OED auxiliary search strategy. We have utilized five benchmark functions, IEEE-30 bus test system, IEEE-57 bus test system, and IEEE-118 bus test system for verifying stability, effectiveness, and optimization performance of

TABLE 7. IEEE test systems characteristics [1].

Items	IEEE-30 bus test system		IEEE-57 bus test system		IEEE-118 bus test system	
	Quantity	Description	Quantity	Description	Quantity	Description
Buses	30	[1]	57	[1]	118	[1]
Branches	41	[1]	80	[1]	186	[1]
Generators	6	Thermal energy sources attached at bus no. 1 (slack/swing), 2, 5, 8, 11 and 13	7	Thermal energy sources attached at bus no. 1 (slack/swing), 2, 3, 6, 8, 9 and 12	54	Thermal energy sources attached at bus no. 1, 4, 6, 8, 10, 12, 15, 18, 19, 24, 25, 26, 27, 31, 32, 34, 36, 40, 42, 46, 49, 54, 55, 56, 59, 61, 62, 65, 66, 69 (slack/swing), 70, 72, 73, 74, 76, 77, 80, 85, 87, 89, 90, 91, 92, 99, 100, 103, 104, 105, 107, 110, 111, 112, 113 and 116
Shunt capacitors	9	On bus no. 10, 12,15, 17, 20, 21, 23, 24 and 29	3	On bus no. 18, 25 and 53	14	On bus no. 5, 34, 37, 44, 45, 46, 48, 74, 79, 82, 83, 105, 107 and 110
Transformer taps	4	On branch no. 11, 12, 15 and 36	17	On branch no. 19, 20, 31, 35, 36, 37, 41, 46, 54, 58, 59, 65, 66, 71, 73, 76 and 80	9	On branch no. 8, 32, 36, 51, 93, 95, 102, 107 and 127
Control variables	24	Active power of generators attached on bus no. 2, 5, 8, 11 and 13, voltage magnitude of all generators, shunt capacitors and transformer taps at selected buses	33	Active power of generators attached on bus no. 2, 3, 6, 8, 9 and 12, voltage magnitude of all generators, shunt capacitors and transformer taps at selected buses	130	Active power all generators (except at swing bus), voltage magnitude of all generators, shunt compensator and transformer tap at selected buses
Connected load	-	283.4 MW	-	1250.8 MW	-	4242 MW
Reactive Power	-	126.2 MVAr	-	336.4 MVAr	-	1439 MVAr
Load buses	24	Voltage [0.95 - 1.05] p.u. on 100 MVA base	50	Voltage [0.94 - 1.06] p.u. on 100 MVA base	64	Voltage [0.94 - 1.06] p.u. on 100 MVA base

proposed IBSA. We have used MATLAB R2017a for implementing IBSA, original BSA and other approaches such as ABC, PSO, DE, and HSA. The MATPOWER 6.0 software package integrated with MATLAB R2017a was utilized for power flow calculation. The simulation and statistical results were measured and a comparison was made with original BSA and other metaheuristic approaches such as DE, PSO, ABC, and HSA. Laptop has Intel(R) Core^{TM} i7-5500U CPU @ 2.40GHz 2.40 GHz and installed RAM @8.00 GB and Microsoft Windows 10 64-bits has been used for the simulation purpose.

In order to measure the optimization performance of proposed IBSA, we have evaluated it on five benchmark functions of different characteristics. The benchmark functions are listed in Table 6 and dimension value is set to be 200 in each function. To verify the efficiency and effectiveness of proposed IBSA on benchmark functions, we have selected the original BSA for comparison. In Figure 2, the simulation results are reported for algorithms' convergence properties on selected benchmark functions. The proposed IBSA has exhibited competitive performance on *Griewank*, *Rosenbrock*, and *Sphere* functions to find global optimum value. It is observed that the proposed IBSA has better convergence, efficiency, and robustness features than the original BSA.

We have conducted ten case studies for measuring stability and performance of the proposed IBSA to solve OPF problems in small-scale to large-scale thermal energy-based power systems. In these case studies, we have considered four objective functions - minimizing electricity generation cost (i.e. regular quadratic fuel cost and valve-point loading effects fuel cost), emission pollution, and active (real) power loss in thermal power systems. Experimental results and statistical analysis of 10 case studies on three standard IEEE test systems are given in the following section.

TABLE 8. IEEE-30 bus test system - fuel cost and emission coefficients [14].

Energy source	Bus no.	Fuel cost coefficients				
		a	b	c	d	e
G_1	1	0	2	0.00375	18	0.037
G_2	2	0	1.75	0.0175	16	0.038
G_5	5	0	1	0.0625	14	0.04
G_8	8	0	3.25	0.00834	12	0.045
G_{11}	11	0	3	0.025	13	0.042
G_{13}	13	0	3	0.025	13.5	0.041

Energy source	Bus no.	Emission coefficients				
		α	β	γ	ω	μ
G_1	1	4.091	-5.554	6.49	0.0002	2.857
G_2	2	2.543	-6.047	5.638	0.0005	3.333
G_5	5	4.258	-5.094	4.586	0.000001	8
G_8	8	5.326	-3.55	3.38	0.002	2
G_{11}	11	4.258	-5.094	4.586	0.000001	8
G_{13}	13	6.131	-5.555	5.151	0.00001	6.667

A. IEEE-30 BUS TEST SYSTEM

In initial four case studies (i.e. case study 1 to case study 4), the standard IEEE-30 bus test system has been utilized for verifying the performance accuracy and effectiveness of IBSA in a small-scale power system. It has active power 283.4 MW (2.834 p.u.) demand and reactive power 126.2 MVAr (1.262 p.u.) demand. Its data and characteristics are specified in Table 7 and further details can be found in study [1]. There are 24 control or decision variables including 5 generators active power output (except swing bus), all 6 generators' voltage magnitude, 9 shunt compensators, and 4 transformer taps. The voltage magnitude limits of generators and load buses are kept in range [0.95 1.05] p.u. and [0.95 1.1] p.u., respectively.

1) CASE STUDY 1: MINIMIZING QUADRATIC FUEL COST

The OPF problem's primary objective is to minimize generators' fossil fuel cost ($/h) for producing the electricity based on regular quadratic objective function f_1 (13). Energy

TABLE 9. Simulation results of case studies 1 and 2 on IEEE-30 bus test system.

Control variables	Range	Case study 1: Minimization of fuel cost						Case study 2: Minimization of fuel cost with valve-point effect					
		IBSA	BSA	DE	PSO	ABC	HSA	IBSA	BSA	DE	PSO	ABC	HSA
P_{G2} (MW)	[20 80]	48.7145	49.2616	48.7909	48.9971	48.7204	47.4937	44.4761	41.6874	44.9752	49.6048	42.5023	39.9103
P_{G5} (MW)	[15 50]	21.3766	21.3824	21.4098	21.4862	21.3861	21.7700	18.7530	16.3145	18.3806	15	18.8874	20.3057
P_{G8} (MW)	[10 35]	21.2188	20.4812	21.1246	21.9370	21.2326	17.4468	10	16.2795	10.0039	10	11.3847	11.9537
P_{G11} (MW)	[10 30]	11.9239	12.5738	11.9508	10	11.9166	13.7208	10.0022	11.0654	10.0047	10	10	11.5736
P_{G13} (MW)	[12 40]	12	12	12	12	12	12.7600	12	12.1737	12	12	12.9557	13.1903
V_1 (p.u.)	[0.95 1.1]	1.0838	1.0851	1.0839	1.0786	1.0814	1.0581	1.0805	1.0776	1.0850	1.0375	1.0714	1.0563
V_2 (p.u.)	[0.95 1.1]	1.0647	1.0378	1.0649	1.0595	1.0626	1.0461	1.0581	1.0585	1.0619	1.0130	1.0474	1.0322
V_5 (p.u.)	[0.95 1.1]	1.0336	1.0393	1.0336	1.0277	1.0317	1.0184	1.0243	1.0561	1.0281	0.95	1.0208	1.0099
V_8 (p.u.)	[0.95 1.1]	1.0383	1.0346	1.0383	1.0330	1.0364	1.0069	1.0338	1.0317	1.0361	0.9807	1.0282	1.0848
V_{11} (p.u.)	[0.95 1.1]	1.0810	1.0553	1.0873	0.95	1.0946	1.0217	1.0590	1.0537	1.0897	1.1	1.0696	1.0201
V_{13} (p.u.)	[0.95 1.1]	1.0406	1.0428	1.0437	1.1	1.0548	1.0277	1.0650	1.0592	1.0549	0.95	1.0766	1.0667
Q_{c10} (MVAr)	[0 5]	5	4.4861	1.4910	0	2.8537	4.2034	5	2.6433	5	0	5	3.1996
Q_{c12} (MVAr)	[0 5]	4.2745	4.9819	1.2007	0	0	4.3327	5	2.4942	0.0034	5	4.9139	3.0004
Q_{c15} (MVAr)	[0 5]	3.7546	1.5426	4.1043	3.0126	3.9257	3.5678	5	1.6647	3.8135	0	5	2.7138
Q_{c17} (MVAr)	[0 5]	4.9999	2.8036	5	0	5	2.3204	5	0.1694	5	5	5	4.5963
Q_{c20} (MVAr)	[0 5]	4.0215	4.2474	4.2008	0	3.8813	4.9025	4.3774	1.6062	3.9775	5	4.2495	3.2355
Q_{c21} (MVAr)	[0 5]	5	2.1105	4.9984	5	5	1.8086	5	2.1155	5	5	5	1.2258
Q_{c23} (MVAr)	[0 5]	2.9689	4.0812	2.8275	5	2.7926	1.4554	5	2.4121	2.5369	5	2.7446	3.7076
Q_{c24} (MVAr)	[0 5]	5	4.0190	4.9899	0	5	3.8810	5	2.1160	5	5	5	3.1557
Q_{c29} (MVAr)	[0 5]	2.4366	2.6661	2.3734	5	2.2213	3.5505	2.5404	0.7494	2.5270	0	2.4516	1.6686
T_{11} (p.u.)	[0.9 1.1]	1.0126	0.9534	1.0525	0.9707	1.0774	0.9926	1.0386	0.9984	1.0249	1.009	0.9971	1.0091
T_{12} (p.u.)	[0.9 1.1]	0.9770	1.0761	0.9225	0.9	0.9	0.9460	0.9396	1.0490	0.9886	0.9	0.9684	1.0897
T_{15} (p.u.)	[0.9 1.1]	0.9662	1.0314	0.9648	1.0477	0.9795	1.0262	1.0112	1.0522	0.9759	0.9	1.0284	1.0453
T_{36} (p.u.)	[0.9 1.1]	0.9738	0.9868	0.9731	0.9777	0.9718	0.9647	0.9878	0.9522	0.9787	0.9	0.9667	0.9532
State variables and parameters													
P_{G1} (MW)	[50 200]	177.16277	176.95956	177.11977	178.25196	177.14156	179.86083	198.85353	196.73864	198.68198	199.13298	198.38781	197.59449
Q_{G1} (MVAr)	[-20 150]	2.69059	25.82336	2.68720	-0.90316	0.60742	-17.25271	1.50142	-6.32686	5.79981	13.29559	2.00799	-0.60683
Q_{G2} (MVAr)	[-20 60]	20.10741	-20	20.35496	18.90873	17.31498	28.79175	12.40395	3.25166	14.58834	39.78293	0.4434	-8.07769
Q_{G5} (MVAr)	[-15 62.5]	25.55891	40.03170	25.38722	27.11731	24.88422	28.81415	22.30349	56.66535	22.99489	3.42775	27.56737	27.78952
Q_{G8} (MVAr)	[-15 48.7]	32.80059	32.80059	27.64679	38.11267	23.20047	48.7	27.75564	22.20115	27.36748	38.57959	29.06624	48.7
Q_{G11} (MVAr)	[-10 40]	16.25831	5.04806	23.93212	-10	29.37808	0.37109	12.49753	13.81813	22.55452	34.61831	11.1122	8.04698
Q_{G13} (MVAr)	[-15 44.7]	-6.94745	13.25851	-4.63822	39.24385	2.90680	9.54657	11.54638	28.32962	3.86903	-15	20.47395	34.83518
P_D (MW)		283.4	283.4	283.4	283.4	283.4	283.4	283.4	283.4	283.4	283.4	283.4	283.4
P_G (MW)		292.3965	292.6586	292.3959	292.6722	292.3972	293.0521	294.0848	294.2591	294.0464	295.7377	294.1179	294.5281
P_{loss} (MW)		8.9965	9.2586	8.9959	9.2722	8.9972	9.6521	10.6848	10.8591	10.6464	12.3377	10.7179	11.1281
Voltage deviation (p.u.)		0.92389	0.45639	0.92158	0.79384	0.94569	0.31239	0.81467	0.39253	0.85351	0.67178	0.87181	0.32430
Emission (ton/h)		0.36633	0.36567	0.36622	0.36989	0.36628	0.37307	0.43814	0.42957	0.43762	0.44054	0.43574	0.43169
Fuel cost ($/h)		**800.3975**	801.3396	800.3978	801.1773	800.4040	802.3204	832.1423	836.6486	**832.0568**	838.2431	832.8819	835.8461

TABLE 10. Simulation results of case studies 3 and 4 on IEEE-30 bus test system.

| Algorithm	P_{loss} (MW)	P_G (MW)	Fuel cost ($/h)	Emission (ton/h)	Voltage deviation (p.u.)
Case study 3: Minimizing active power loss					
IBSA	3.0951	286.4951	1027.4002	0.20727	0.90383
BSA	3.1714	286.5714	1027.6328	0.20728	0.46360
DE	**3.0828**	286.4829	1027.3620	0.20726	0.91058
PSO	3.1545	286.5545	1027.5810	0.20727	0.93267
ABC	3.0830	286.4835	1027.3652	0.20726	0.91560
HSA	3.3961	287.1109	1005.4364	0.20794	0.34839
Case study 4: Minimizing emission pollution					
IBSA	3.2907	286.6907	1015.6857	0.20484	0.90570
BSA	3.9530	287.3530	1030.0347	0.20739	0.49478
DE	3.2177	286.6177	1015.4273	**0.20482**	0.90409
PSO	3.4315	286.8315	1016.1882	0.20488	0.99724
ABC	3.2671	286.6671	1015.6162	0.20483	0.85700
HSA	3.9707	287.3707	1011.7692	0.20681	0.43134

sources or generators' fuel cost coefficients are given in Table 8, which are taken from study [14]. The minimum electricity generation cost of fossil fuel energy sources achieved from the proposed IBSA was **800.3975** $/h to fulfill the active load demand, which was less than the fuel cost or electricity generation cost obtained from original BSA and all other algorithms. The optimal values of control variables, state variables, and objective function's parameters achieved by all algorithms are specified in Table 9, while minimum electricity generation cost is shown in **boldface**.

2) CASE STUDY 2: MINIMIZING VALVE-POINT LOADING EFFECTS QUADRATIC FUEL COST

The OPF problem's objective function - reducing electricity generation cost ($/h) f_2 defined in (14) was considered, in this case study. In Table 8, cost coefficients of fossil fuel for thermal energy sources are specified. To fulfill active load demand in system, fossil fuel cost 832.1597 $/h to generate electricity from thermal generators (energy sources) was obtained from the proposed IBSA, which was less than the power generation cost of original BSA and close to minimum power generation cost **832.0568** $/h obtained from DE. The optimization results are specified in Table 9 for this case study.
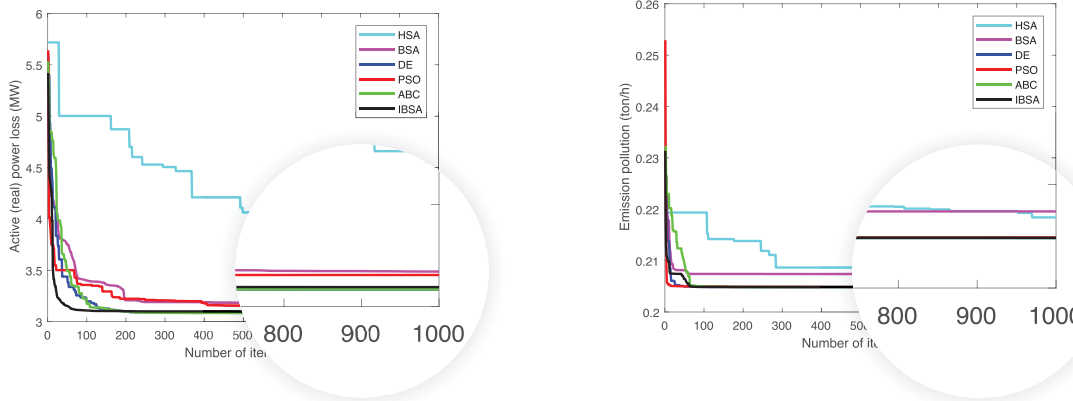
3) CASE STUDY 3: MINIMIZING ACTIVE POWER LOSS

The objective function f_3 of the OPF problem defined in (15) was under consideration for the active power loss P_{loss} reduction in the power system. In which fuel cost function f_2 defined in (14) was considered for calculating electricity generation cost. The active power loss P_{loss} in the power system for proposed IBSA approach was 3.0951 MW close to minimum power loss **3.0828** MW obtained from DE. The optimization results are given in Table 10 for this case study.
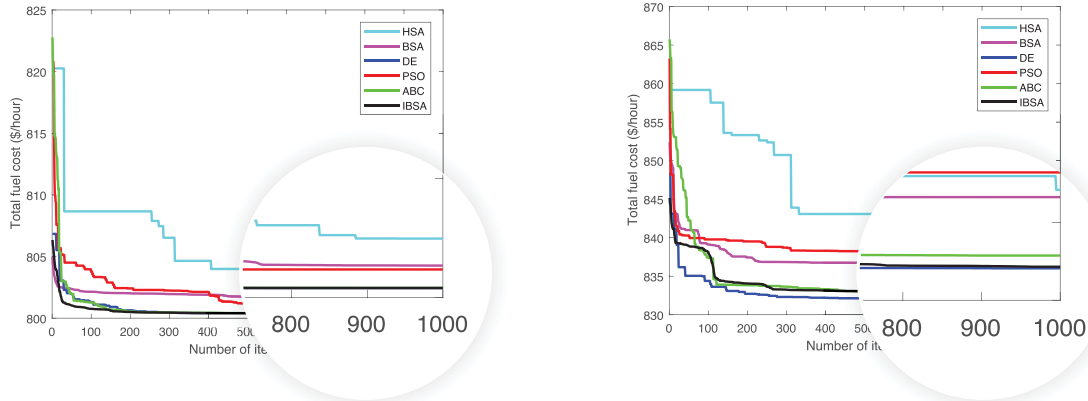
(a) Case study 1: Minimizing fuel cost

(b) Case study 2: Minimizing fuel cost with valve-point effect

(c) Case study 3: Minimizing power loss in system

(d) Case study 4: Minimizing emission pollution

FIGURE 3. Algorithms' convergence properties on IEEE-30 bus test system.
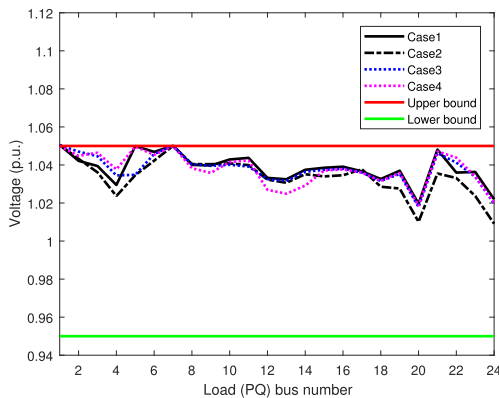

FIGURE 4. Load buses' voltage magnitude profile for IBSA on IEEE-30 bus test system.

4) CASE STUDY 4: MINIMIZING EMISSION POLLUTION

Based on the function f_4 (16), the objective was set as reduction of emission pollution in this case study. In Table 8, the emission coefficients for thermal energy sources are provided. The amount of emission pollution in case of

proposed IBSA was 0.20484 ton/h, which is close to minimum emission **0.20482** ton/h polluted in case of DE approach and less than in case of original BSA. In Table 10, the simulation results of case study 4 are specified.

A comparison is made between simulation results achieved using the proposed IBSA, original BSA, and other meta-heuristic approaches to solve the OPF problems. In Figure 3, algorithms' convergence profiles are graphically plotted for four case studies on the IEEE-30 bus test system.

The summary of statistical results for each case study on IEEE-30 bus test system (i.e. case study 1 to case study 4) conducted with IBSA, original BSA, and other search algorithms is shown in Table 11. In each case study, the columns min, max, and average indicate the objective function values (i.e. best, worst, mean). The column time(s) indicates the execution time in seconds for a single run is taken to obtain the feasible solution (best result). In case study 1, the best fuel cost (minimum) **800.3975** $/h is obtained from IBSA, with the worst fuel cost (maximum) 800.3978 $/h, the mean 800.3976 $/h, and standard deviation 0.0001. It is observed that no single approach is capable of

TABLE 11. Statistical summary on IEEE-30 bus test system.

Algorithm	Min($/h)	Max($/h)	Average($/h)	Standard deviation(σ)	Time (s)
Case study 1: Minimization of fuel cost					
IBSA	**800.3975**	800.3978	800.3976	0.0001	521.86
BSA	801.3396	801.3402	801.3398	0.0002	468.23
DE	800.3978	800.4000	800.3987	0.0012	349.34
PSO	801.1773	801.1773	801.1773	0	652.42
ABC	800.4040	800.5000	800.4379	0.0538	499.62
HSA	802.3204	802.3204	802.3204	0	11.23
Case study 2: Minimization of fuel cost with valve-point effect					
IBSA	832.1423	832.1597	832.1510	0.0123	669.05
BSA	836.6486	836.7052	836.6769	0.0400	332.80
DE	**832.0568**	832.0568	832.0568	0	331.50
PSO	838.2431	838.2431	838.2431	0	543.46
ABC	832.8819	833.0035	832.9427	0.0860	571.34
HSA	835.8461	836.8257	836.3359	0.6927	13.57
Case study 3: Minimizing active power loss					
IBSA	3.0951	3.0951	3.0951	0	493.24
BSA	3.1714	3.1715	3.1715	0.0001	302.64
DE	**3.0828**	3.0828	3.0828	0	368.68
PSO	3.1545	3.1545	3.1545	0	472.53
ABC	3.0830	3.0842	3.0834	0.0011	407.39
HSA	3.3961	3.4325	3.4143	0.0257	12.36
Case study 4: Minimizing emission pollution					
IBSA	0.20484	0.20484	0.20484	0	917.85
BSA	0.20739	0.20745	0.20742	4.24×10^{-5}	636.43
DE	**0.20482**	0.20482	0.20482	0	344.40
PSO	0.20488	0.20492	0.20489	1.41×10^{-5}	826.19
ABC	0.20483	0.20490	0.20488	7.07×10^{-5}	488.22
HSA	0.20681	0.20720	0.20701	0.0003	10.84

TABLE 12. IEEE-57 bus test system - fuel cost and emission coefficients [14].

Energy source	Bus no.	a	b	c	d	e
Fuel cost coefficients						
G_1	1	0	20	0.07758	18	0.037
G_2	2	0	40	0.01	16	0.038
G_3	3	0	20	0.25	13.5	0.041
G_6	6	0	40	0.01	18	0.037
G_8	8	0	20	0.02222	14	0.04
G_9	9	0	40	0.01	15	0.039
G_{12}	12	0	20	0.03226	12	0.045

Energy source	Bus no.	α	β	γ	ω	μ
Emission coefficients						
G_1	1	4.091	-5.554	6.49	0.0002	0.286
G_2	2	2.543	-6.047	5.638	0.0005	0.333
G_3	3	6.131	-5.555	5.151	0.00001	0.667
G_6	6	3.491	-5.754	6.39	0.0003	0.266
G_8	8	4.258	-5.094	4.586	0.000001	0.8
G_9	9	2.754	-5.847	5.238	0.00040	0.288
G_{12}	12	5.326	-3.555	3.380	0.002000	0.200

providing feasible or best mean feasible solutions in all the case studies. In case of the execution time for a single run, it is evident that IBSA spends more execution time than the original BSA and other algorithms. The IBSA demonstrated faster convergence in case studies 1, 3, and 4. The load buses voltage magnitude profiles shown in Figure 4 are measured during performance evaluation of proposed IBSA approach in above four case studies.

B. IEEE-57 BUS TEST SYSTEM
The standard IEEE-57 bus test system has capacity of 1250.8 MW (12.508 p.u.) active power demand and 336.4 MVAr (3.364 p.u.) reactive power demand. It is utilized for simulation purposes and its detailed characteristics can be found in Table 7. There are 33 control variables including 6 energy sources, active power output (except swing bus), all 7 load buses voltage magnitude, 3 shunt compensators, and 17 transformer taps. The voltage magnitude of generators and load buses are kept in range [0.94 1.06] p.u. and [0.95 1.1] p.u., respectively. In case studies (i.e. case study 5 to case study 8), the optimizing features of the proposed IBSA are measured on the IEEE-57 bus system to solve OPF problems.

1) CASE STUDY 5: MINIMIZING QUADRATIC FUEL COST
In this case study, the objective function f_1 of the OPF problem defined in (13) was under consideration for electricity generation cost reduction in the power system. The fossil fuel cost coefficients related to energy sources for calculating power generation cost are specified in Table 12. To accomplish active load demand in the power system, minimum power generation cost or fossil fuel cost **41663.5500** $/h was achieved by applying the proposed IBSA. The simulation results including values of the power generation cost, control variables, state variables, and other parameters obtained using all optimization approaches in case study 5 are specified in Table 13, while minimum power generation cost or fossil fuel cost is shown in **boldface**.

2) CASE STUDY 6: MINIMIZING VALVE-POINT LOADING EFFECTS QUADRATIC FUEL COST
In this case study, we have included the valve-point loading effect cost factor in the regular quadratic fuel cost curve for measuring the power output cost. The OPF problem's objective function f_2 defined in (14) was studied to reduce the power output cost. In Table 12, cost coefficients of fossil fuel related to IEEE-57 bus system energy sources for calculating power generation cost are specified. To fulfill active load demand in the power system, power generation cost 41737.8360 $/h was obtained from the IBSA approach, which is close to optimal total power generation cost **41736.8566** $/h achieved using the DE algorithm. However, IBSA performed better than the original BSA. In Table 13, simulation results for case study 6 are specified.

3) CASE STUDY 7: MINIMIZING ACTIVE POWER LOSS
The OPF problem's objective function f_3 defined in (15) is studied for evaluating performance of the proposed IBSA approach. The OPF objective function f_2 defined in (14) was considered for calculating the power output fuel cost. In this study the objective is to reduce total active (real) power loss in the power system. A comparison is made between simulation results achieved using the proposed IBSA, original BSA, and other metaheuristic approaches to solve the OPF problems. The DE optimization approach was performed better as compared to all other algorithms and power loss **9.9041** MW was achieved. Total power loss 10.1426 MW was obtained from proposed IBSA and its performance was better than original BSA, PSO, and HSA. The simulation results for case study 7 are available in Table 14.

TABLE 13. Simulation results of case studies 5 and 6 on IEEE-57 bus test system.

Control variables	Range	Case study 5: Minimizing fuel cost						Case study 6: Minimizing fuel cost with valve-point effect					
		IBSA	BSA	DE	PSO	ABC	HSA	IBSA	BSA	DE	PSO	ABC	HSA
P_{G2} (MW)	[30 100]	90.0565	85.3753	90.9992	64.1733	88.6093	93.8473	100	84.6215	99.8173	41.9816	100	79.9001
P_{G3} (MW)	[40 140]	44.9974	45.4740	44.8451	44.3100	45.0385	47.7317	43.5888	44.0133	43.4434	40	43.5492	52.765
P_{G6} (MW)	[30 100]	70.6406	85.3638	70.4918	59.3306	72.4884	73.4751	51.4055	84.8159	52.1103	100	52.0912	70.3484
P_{G8} (MW)	[100 550]	460.6991	470.1719	459.8915	449.2528	460.8890	522.2746	464.3496	471.0809	462.769	432.7485	464.1679	459.677
P_{G9} (MW)	[30 100]	96.4542	85.9428	98.0141	100	94.5041	81.7758	100	86.3928	100	100	100	82.6784
P_{G12} (MW)	[100 410]	359.9466	351.2972	359.0412	410	360.8654	326.4927	362.5797	352.5116	363.6357	410	362.3473	383.2611
V_1 (p.u.)	[0.95 1.1]	1.0709	1.0658	1.0710	0.95	1.0713	1.0311	1.0728	1.0530	1.0749	0.9549	1.0669	1.0013
V_2 (p.u.)	[0.95 1.1]	1.0885	1.0635	1.0864	0.95	1.0741	0.9827	1.1	1.0553	1.0878	0.95	1.0666	1.0013
V_3 (p.u.)	[0.95 1.1]	1.0613	1.0649	1.0610	1.1	1.0615	0.9793	1.0927	1.0522	1.0629	1.1	1.0568	1.0866
V_6 (p.u.)	[0.95 1.1]	1.0651	1.0652	1.0409	0.95	0.95	1.0372	1.0155	1.0522	1.0522	0.9927	1.0617	1.0934
V_8 (p.u.)	[0.95 1.1]	1.0808	1.0655	1.0811	1.0088	1.0805	1.0751	1.0812	1.0524	1.0811	1.0114	1.0798	1.0147
V_9 (p.u.)	[0.95 1.1]	1.0770	1.0682	1.0845	1.1	1.1	1.0667	1.0609	1.0512	1.1	1.1	1.1	0.9613
V_{12} (p.u.)	[0.95 1.1]	1.0561	1.0667	1.0558	0.9644	1.0570	1.0509	1.0577	1.0967	1.0585	0.9657	1.0508	1.0513
Q_{c18} (MVAr)	[0 20]	8.3299	17.1618	9.7575	20	8.6704	15.7035	0.0004	17.3082	6.4877	20	11.1897	10.9046
Q_{c25} (MVAr)	[0 20]	13.3913	17.1469	12.6434	20	14.6934	7.3462	13.1664	17.2032	14.2887	12.7418	15.6066	5.8359
Q_{c53} (MVAr)	[0 20]	12.0776	8.9803	11.8204	13.7043	12.0694	16.3140	12.0443	5.0598	11.5656	20	12.3021	4.0821
T_{19} (p.u.)	[0.9 1.1]	1.0457	1.0099	1.0895	1.1	1.0388	0.9638	1.0927	1.0049	0.9194	1.1	0.9816	1.0222
T_{20} (p.u.)	[0.9 1.1]	0.9543	1.0087	0.9572	0.9	0.9609	1.0765	0.9	1.0017	1.0605	0.9	1.0091	1.0256
T_{31} (p.u.)	[0.9 1.1]	1.0099	1.0122	1.0235	1.0430	1.0095	0.9644	1.0091	0.9995	1.0137	1.0404	1.0094	0.9432
T_{35} (p.u.)	[0.9 1.1]	1.0146	1.0047	0.9991	1.0079	0.9719	0.9327	1.0217	0.9870	1.0280	0.9	0.9775	0.9092
T_{36} (p.u.)	[0.9 1.1]	1.0139	1.0030	1.0195	1.1	1.0850	1.0066	1.0009	0.9932	1.0169	1.1	1.0952	1.0738
T_{37} (p.u.)	[0.9 1.1]	1.0323	0.9995	1.0285	1.0013	1.0330	1.0080	1.0288	1.0061	1.0319	1.0029	1.0297	1.0635
T_{41} (p.u.)	[0.9 1.1]	0.9996	1.0037	0.9980	0.9322	0.9998	1.0002	0.9994	0.9933	0.9991	0.9377	0.9989	0.9341
T_{46} (p.u.)	[0.9 1.1]	0.9631	1.0045	0.9636	0.9	0.9633	0.9263	0.9612	0.9932	0.9546	0.9	0.9617	0.9243
T_{54} (p.u.)	[0.9 1.1]	0.9173	1.0073	0.9163	0.9	0.9179	1.0181	0.9192	0.9943	0.9194	0.9	0.927	0.9471
T_{58} (p.u.)	[0.9 1.1]	0.9847	1.0081	0.9856	0.9	0.9852	0.9249	0.9883	0.9981	0.9874	0.9	0.9815	0.9223
T_{59} (p.u.)	[0.9 1.1]	0.9701	1.0209	0.9673	0.9	0.9711	0.9305	0.9730	0.9998	0.9737	0.9	0.9629	0.9134
T_{65} (p.u.)	[0.9 1.1]	0.9802	0.9995	0.9797	0.9	0.9807	1.0351	0.9819	0.9984	0.9828	0.9	0.9764	0.978
T_{66} (p.u.)	[0.9 1.1]	0.9430	0.9998	0.9426	0.9	0.9438	1.0105	0.9453	0.9931	0.9480	0.9	0.9375	0.9001
T_{71} (p.u.)	[0.9 1.1]	0.9787	1.0085	0.9809	0.9	0.9790	0.9658	0.9807	1.0014	0.9847	0.9	0.972	0.9943
T_{73} (p.u.)	[0.9 1.1]	0.9929	1.0041	0.9916	0.9957	0.9926	0.9819	0.9924	0.9842	0.9941	0.9965	0.9964	1.0904
T_{76} (p.u.)	[0.9 1.1]	0.9664	1.0094	0.9608	0.9705	0.9665	0.9419	0.9660	1.0024	0.9679	0.9700	0.979	0.9806
T_{80} (p.u.)	[0.9 1.1]	1.0061	1.0047	1.0055	0.9193	1.0067	1.0531	1.0052	0.9931	1.0027	0.9292	0.9997	0.9517
State variables and parameters													
P_{G1} (MW)	[0 575.88]	142.75453	143.81046	142.27938	139.09814	143.14905	127.19649	143.59106	145.05535	143.64386	141.40456	143.37331	139.85680
Q_{G1} (MVAr)	[-140 200]	44.55473	25.23516	45.45106	-4.1525	44.21742	92.9895	35.63403	-6.51829	47.74854	15.63567	44.31363	-13.8731
Q_{G2} (MVAr)	[-17 50]	50	40.17199	50	41.08236	50	-17.0000	50	50	50	28.75933	50	39.53958
Q_{G3} (MVAr)	[-10 60]	34.14049	47.00451	33.33201	60	33.22103	-10	60	34.52854	35.45944	60	29.09894	60
Q_{G6} (MVAr)	[-8 25]	-8	1.65751	-8	-8	-8	-8	-8	2.136	-8	-8	-6.94961	25
Q_{G8} (MVAr)	[-140 200]	51.80449	13.39149	52.90497	82.73297	50.11582	79.91493	50.6939	-2.50846	51.64197	78.02735	56.544	17.83341
Q_{G9} (MVAr)	[-3 9]	9	9	9	9	9	9	9	9	9	9	9	-3
Q_{G12} (MVAr)	[-150 155]	55.91166	96.48863	55.65756	64.18258	57.21871	122.08419	53.06243	155	54.04049	60.89133	50.26178	155
P_D (MW)		1250.8	1250.8	1250.8	1250.8	1250.8	1250.8	1250.8	1250.8	1250.8	1250.8	1250.8	1250.8
P_G (MW)		1265.5490	1267.4354	1265.5623	1266.1648	1265.5439	1272.7936	1265.5146	1268.4913	1265.4195	1266.1347	1265.5289	1268.4869
P_{loss} (MW)		14.7490	16.6354	14.7623	15.3648	14.7439	21.9936	14.7146	17.6913	14.6195	15.3347	14.7289	17.6869
Voltage deviation (p.u.)		1.78007	1.45812	1.72444	1.55136	1.78893	1.01438	1.80284	1.34429	1.77513	1.48578	1.78545	1.20028
Emission (ton/h)		1.35663	1.37572	1.35226	1.41498	1.35889	1.51474	1.37951	1.38305	1.37587	1.37821	1.37812	1.38986
Fuel cost ($/h)		**41663.5500**	41719.4923	41664.3488	41869.6251	41663.6177	41836.2382	41737.8271	41845.7873	**41736.8566**	41974.8183	41737.1023	41913.2283

**TABLE 14.** Simulation results of case studies 7 and 8 on IEEE-57 bus test system.

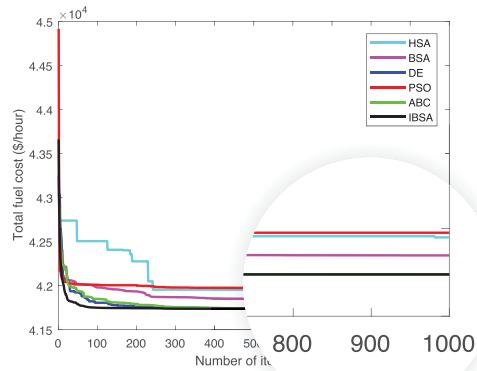|	Case study 7: Minimizing active power loss				
Algorithm	P_{loss} (MW)	P_G (MW)	Fuel cost ($/h)	Emission (ton/h)	Voltage deviation (p.u.)
IBSA	10.1363	1260.9426	44742.0963	1.10525	1.63161
BSA	11.5261	1262.3261	43041.1637	1.14382	1.45101
DE	**9.9041**	1260.7041	44663.2282	1.10502	1.70723
PSO	12.9319	1263.7319	45104.3684	1.10465	1.37874
ABC	9.9287	1260.7287	44593.4956	1.10888	1.69280
HSA	15.1188	1265.3334	42100.1793	1.31747	1.19726
	Case study 8: Minimizing emission pollution				
IBSA	13.4650	1264.2650	45230.9964	0.95797	1.52220
BSA	13.6564	1264.4564	45554.3101	0.97984	1.28967
DE	12.8727	1263.6727	45231.2729	**0.95672**	1.60878
PSO	16.3345	1267.1345	45353.8787	0.96382	1.59944
ABC	13.3469	1264.1469	45217.7225	0.95773	1.07599
HSA	16.3431	1267.1431	42746.7988	1.13636	1.06975

4) CASE STUDY 8: MINIMIZING EMISSION POLLUTION

In this case study, we have used the objective function f_4 defined in (16) for verifying the optimization performance of the proposed IBSA. The main objective is to control the emission of harmful gases into the environment. In Table 12, emission coefficients of thermal generators (energy sources) are given for the IEEE-57 bus test system [14]. The valve-point loading effects are included in the regular quadratic fuel cost for calculating the power generation cost. In this case study the DE approach was performed well as compared to all algorithms and minimum emission pollution **0.95672** ton/h was achieved from the DE approach. The optimal values of objective function - emission pollution, active power loss P_{loss} fossil fuel cost, active power output P_G, and voltage deviation for case study 8 are given in Table 14.

A comparison is made between simulation results achieved using the proposed IBSA, original BSA, and other metaheuristic approaches to solve the OPF problems. In Figure 5, algorithms' convergence profiles of the IEEE-57 bus system for case studies 5, 6, 7, and 8 are shown. The better convergence property of IBSA is shown in Figure 5, in which
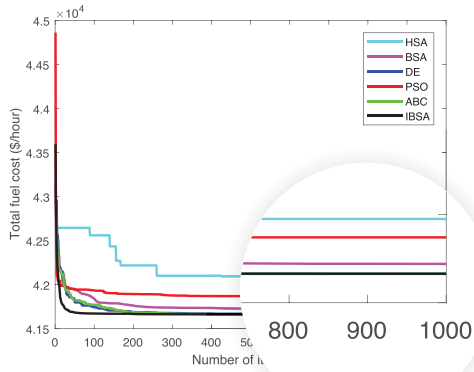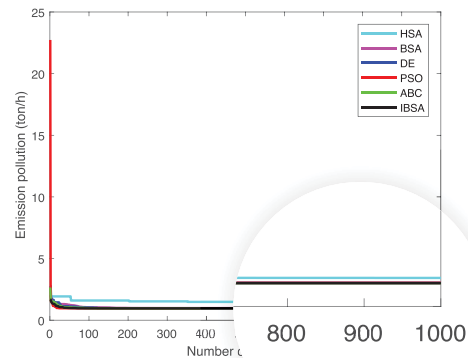
(a) Case study 5: Minimizing fuel cost

(b) Case study 6: Minimizing fuel cost with valve-point effect
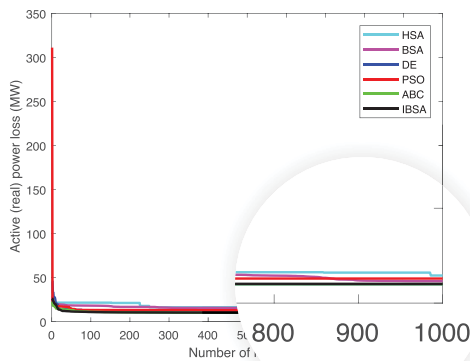
(c) Case study 7: Minimizing power loss in system

(d) Case study 8: Minimizing emission pollution

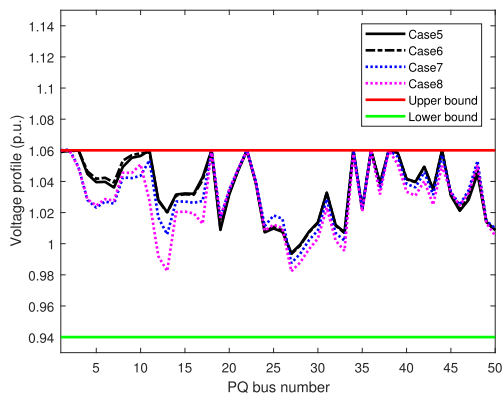**FIGURE 5.** Algorithms' convergence properties on IEEE-57 bus test system.

FIGURE 6. Load buses' voltage magnitude profile for IBSA on IEEE-57 bus test system.

IBSA demonstrates to be more robust. In Figure 6, load buses' voltage magnitude profiles on IEEE-57 bus system for every case study achieved using the proposed IBSA approach are plotted.

In the IEEE-57 bus test system, each case study (i.e. case study 5 to case study 8) was executed 30 times independently to calculate statistical results for the proposed IBSA, original BSA and other approaches. The comparison of statistical analysis is given in Table 15, where the min, max, average, standard deviation (σ), and execution time for a single run are given and the best result is shown in **boldface**. In case study 5, minimum fossil fuel cost (power generation cost) **41663.5500** $/h, was achieved, with maximum fuel cost 41663.5510 $/h, average fuel cost 41663.5510 $/h, and standard deviation 0.0007, by applying the proposed IBSA as compared to original BSA and other optimization approaches. It is observed that IBSA takes more execution time for single run as compared to original BSA and other approaches for finding objective function minimum value (i.e. power generation cost) in each case study on IEEE-57 bus test system.

C. IEEE-118 BUS TEST SYSTEM
The last two case studies 9 and 10 were conducted for measuring optimization performance of the proposed IBSA

TABLE 15. Statistical summary on IEEE-57 bus test system.

Algorithm	Case study 5: Minimization of fuel cost				
	Min($/h$)	Max($/h$)	Average($/h$)	Standard deviation(σ)	Time (s)
IBSA	**41663.5500**	41663.5510	41663.5510	0.0007	1943.06
BSA	41719.4923	41719.5683	41719.5300	0.0537	565.96
DE	41664.3488	41664.3500	41664.3490	0.0008	961.01
PSO	41869.6251	41869.6251	41869.6251	0	982.70
ABC	41663.6177	41663.6200	41663.6190	0.0016	1617.68
HSA	41836.2382	41836.2396	41836.2390	0.0010	19.10
	Case study 6: Minimization of fuel cost with valve-point effect				
IBSA	41737.8271	41737.8360	41737.8320	0.0063	2105.15
BSA	41845.7873	41845.8912	41845.8390	0.0735	865.88
DE	**41736.8566**	41736.8600	41736.8580	0.0024	912.83
PSO	41974.8183	41974.8183	41974.8183	0	874.52
ABC	41737.1023	14737.1200	14737.1110	0.0125	1170.86
HSA	41913.2283	41913.2283	41913.2283	0	19.08
	Case study 7: Minimizing active power loss				
IBSA	10.1363	10.1427	10.1395	0.0045	2006.76
BSA	11.5261	11.5301	11.5281	0.0028	936.42
DE	**09.9041**	09.9041	09.9041	0	1031.45
PSO	12.9319	12.9319	12.9319	0	885.23
ABC	09.9287	09.9293	09.9290	0.0004	1180.90
HSA	15.1188	15.1188	15.1188	0	19.51
	Case study 8: Minimizing emission pollution				
IBSA	0.95797	0.95800	0.95799	2.83×10^{-5}	2141.90
BSA	0.97984	0.97990	0.97987	4.24×10^{-5}	934.00
DE	**0.95672**	0.95672	0.95672	0	1037.57
PSO	0.96382	0.96394	0.96388	8.48×10^{-5}	1035.34
ABC	0.95773	0.95781	0.95777	5.66×10^{-5}	1250.01
HSA	1.13636	1.13648	1.13642	8.48×10^{-5}	19.63

approach for finding feasible solutions to OPF problems. The IEEE-118 bus system has been utilized for simulation purposes. It has active power 4242 MW (42.42 p.u.) demand and 1439 MVAr (14.39 p.u.) reactive power demand and consists of 130 control variables. In these control variables 53 thermal generators or energy sources' active power output (except energy source attached at swing bus), all 54 load buses voltage magnitudes, 9 transformer taps setting, and 14 shunt compensators are included. The voltage magnitude boundary limits of thermal generators (energy sources) and load buses are kept in range of [0.94 1.06] p.u. and [0.95 1.1] p.u., respectively. Furthermore, details about data and characteristics are presented in Table 7.

1) CASE STUDY 9: MINIMIZING QUADRATIC FUEL COST
The OPF problem's primary objective based on the regular quadratic cost function f_1 (13) to reduce power generation cost is considered for verifying optimization performance and effectiveness of the proposed IBSA approach, in this case study. All thermal power generation units (energy sources) fossil fuel cost coefficients are taken from (Power System Test Case Archive: http://labs.ece.uw.edu/pstca/) for calculating the power generation cost based on a regular quadratic cost curve. The proposed IBSA's performance was best as compared to all other algorithms and minimum total power generation cost **134941.0367** $/h was achieved from the IBSA approach to fulfill active load demand of the system. The simulation results including optimal values of objective

TABLE 16. Simulation results of case studies 9 and 10 on IEEE-118 bus test system.

Algorithm	Case study 9: Minimizing fuel cost			
	P_{loss} (MW)	P_G (MW)	Fuel cost ($/h$)	Voltage deviation (p.u.)
IBSA	57.9943	4299.9943	**134941.0367**	3.22819
BSA	52.8279	4294.8279	141294.5253	2.90292
DE	61.8903	4303.8903	135232.2459	2.22564
PSO	80.3896	4322.3896	142609.1263	3.20931
ABC	58.9133	4300.9133	135156.6378	1.87756
HSA	73.6520	4315.6520	143410.0286	1.46383
	Case study 10: Minimizing active power loss			
IBSA	**16.2869**	4258.2869	155404.2608	3.26716
BSA	41.2285	4283.2285	146486.3203	2.22604
DE	20.6849	4262.9649	151637.4021	0.64632
PSO	41.9524	4283.9524	153664.5997	2.62945
ABC	18.9356	4260.9356	152069.2884	1.59156
HSA	52.0965	4294.0965	157936.0445	1.33972

**TABLE 17.** Statistical summary on IEEE-118 bus test system.

Algorithm	Case study 9: Minimization of fuel cost				
	Min ($/h$)	Max ($/h$)	Average ($/h$)	Standard deviation(σ)	Time (s)
IBSA	**134941.0367**	134941.0367	134941.0367	0	18613.52
BSA	141294.5253	141294.5400	141294.5300	0.0204	5177.34
DE	135232.2459	135232.3041	135232.2800	0.0411	8852.61
PSO	142609.1263	142609.2048	142609.1700	0.0555	7473.17
ABC	135156.6378	135157.0154	135156.8300	0.2670	12662.19
HSA	143410.0286	143410.8142	143410.4200	0.5555	194.32
	Case study 10: Minimizing active power loss				
IBSA	**16.2869**	16.2872	16.2871	0.0002	22614.27
BSA	41.2285	41.2299	41.2292	0.0010	5285.99
DE	20.6849	20.6852	20.6851	0.0003	8513.02
PSO	41.9524	41.9530	41.9529	0.0007	7834.16
ABC	18.9356	18.9370	18.9360	0.0010	11599.18
HSA	52.0965	52.0981	52.0970	0.0011	287.74

function, total power generation P_G, active power loss P_{loss}, and voltage deviation for all algorithms in case study 9 are given in Table 16, while minimum electricity generation cost is shown in **boldface**.

2) CASE STUDY 10: MINIMIZING ACTIVE POWER LOSS
The OPF problem objective function - reducing active power loss f_3 defined in (15) was taken for measuring optimization performance of the IBSA, in this case study. The regular quadratic cost function f_1 (13) was utilized for calculating the power generation cost. The proposed IBSA has performed better than the original BSA and other metaheuristic approaches, in this case study. The minimum total active power loss P_{loss} in transmission lines **16.2869** MW was achieved from the IBSA approach. In Table 16, simulation results including optimal values of objective function P_{loss}, total power output P_G, fuel cost, and voltage deviation obtained from all algorithms are given.

The optimization results for case study 9 and 10 were obtained from IBSA, original BSA, and other metaheuristic approaches and a comparison was made between these results for evaluating the performance of IBSA approach. Figure 7 shows convergence characteristics of IBSA, original BSA, and other metaheuristic approaches for approaching optimal values of the OPF problems' objective functions.
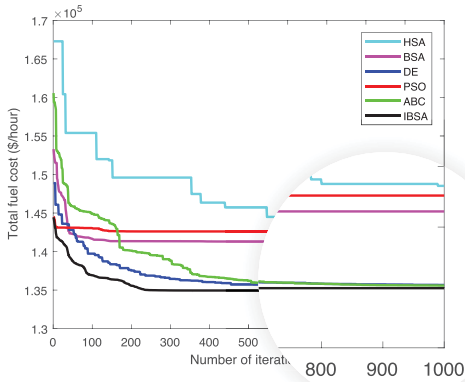
(a) Case study 9: Minimizing fuel cost
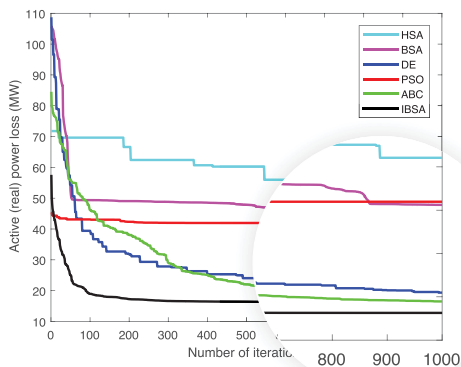
(b) Case 10: Minimizing power loss in system

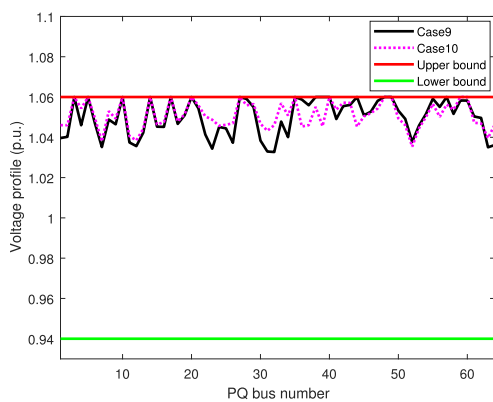**FIGURE 7.** Algorithms' convergence properties on IEEE-118 bus test system.

FIGURE 8. Load buses' voltage magnitude profile for IBSA on IEEE-118 bus test system.

The proposed IBSA approach demonstrated more robust and faster convergence than the original BSA and all other approaches. The Figure 8 shows load buses voltage magnitude profiles for case studies 9 and 10 obtained from the IBSA approach on the IEEE-118 bus test system.

In case studies 9 and 10 simulations were run 30 times independently for the proposed IBSA, original BSA, and other approaches on the IEEE-118 bus system, in order to obtain statistical results. The comparison of statistical results are given in Table 17, where the min, max, average, standard deviation (σ), and execution time for a single run are given and the best result is shown in boldface.

The statistical results of case studies 9 and 10 indicate that the proposed IBSA shows good performance on the best, worst, mean, and standard deviation (σ), when compared with original BSA and other algorithms. In case study 9, the objective function best value (minimum fuel cost) **134941.0367** $/h, worst value (maximum fuel cost) 134941.0367 $/h, and mean value (average fuel cost) 134941.0367 $/h, with standard deviation (σ) 0, were obtained by applying the proposed IBSA. The objective function best value (minimum active power loss) **16.2869** MW, worst value (maximum active power loss) 16.2872 MW, and mean value (average active power loss) 16.2871 MW, with standard deviation (σ) 0.0002, were obtained in proposed IBSA. It is evident that IBSA spends more execution time for single run as compared to original BSA and other approaches for finding objective function minimum or best value in each case study on IEEE-118 bus test system. The proposed IBSA approach takes longer execution time than the original BSA and other metaheuristic approaches, because OL strategy is implemented at each iteration for predicting the optimal solution vector based on improving the ability of exploitation. We used the same parameter settings and the number of iterations (maximum iterations = 1000) in each case study for the proposed IBSA and other algorithms.

V. CONCLUSION

In this research work, we have adopted a search technique based on OL strategy to improve BSA. The OL strategy has significant features to find an optimal solution, in which few experimental test cases are conducted instead of exhaustive experimental test cases for predicting the best combination of decision parameters' values in two candidate solution vectors. We have proposed IBSA to tackle the nonconvex, nonlinear, and quadratic nature of large-scale OPF problems in power systems. In which, to reduce power output cost, emission pollution, and active power loss were set as objectives to address OPF problems. We have utilized IEEE-30 bus test system, IEEE-57 bus test system, and IEEE-118 bus test system, in order to identify improvement due to OL strategy and verifying the stability, optimization performance, and effectiveness of the proposed IBSA. On these standard IEEE test systems simulation and statistical results are measured and a comparison is made to examine optimizing features of the proposed IBSA. By addressing OPF problems in power systems, it has been observed that lowest electricity generation cost **800.3975**$/h on IEEE-30 bus system, **41663.5500**$/h on IEEE-57 bus system, and **134941.0367**$/h on IEEE-118 bus system have been

achieved using proposed IBSA. To address the OPF problem on the IEEE 118-bus system, minimum active power loss **16.2869**MW in transmission lines of the power system has been achieved by applying the proposed IBSA approach. In order to draw convincing conclusions, statistical results indicate that no single approach is capable of finding the best feasible solution of the OPF problem in all case studies. However, statistical and simulation results of most case studies have presented that the IBSA has best efficiency, robustness, and convergence properties as compared to original BSA and other heuristic approaches.

The application of the proposed IBSA may be extended to solve other optimization problems in large-scale thermal power systems including transient stability-constrained OPF, chance-constrained OPF, and unit commitment etc. in future.

REFERENCES

[1] A. E. Chaib, H. R. E. H. Bouchekara, R. Mehasni, and M. A. Abido, "Optimal power flow with emission and non-smooth cost functions using backtracking search optimization algorithm," *Int. J. Elect. Power Energy Syst.*, vol. 81, pp. 64–77, Oct. 2016.

[2] E. P. De Carvalho, A. Dos Santos, and T. F. Ma, "Reduced gradient method combined with augmented Lagrangian and barrier for the optimal power flow problem," *Appl. Math. Comput.*, vol. 200, no. 2, pp. 529–536, Jul. 2008.

[3] F. Capitanescu and L. Wehenkel, "Experiments with the interior-point method for solving large scale optimal power flow problems," *Electric Power Syst. Res.*, vol. 95, pp. 276–283, Feb. 2013.

[4] M. Pourakbari-Kasmaei, M. Lehtonen, M. Fotuhi-Firuzabad, M. Marzband, and J. R. S. Mantovani, "Optimal power flow problem considering multiple-fuel options and disjoint operating zones: A solver-friendly MINLP model," *Int. J. Electr. Power Energy Syst.*, vol. 113, pp. 45–55, Dec. 2019.

[5] S. Tu, A. Wachter, and E. Wei, "A two-stage decomposition approach for AC optimal power flow," *IEEE Trans. Power Syst.*, vol. 36, no. 1, pp. 303–312, Jan. 2021.

[6] B. Liu, J. Li, H. Ma, and Y. Liu, "Generalized benders decomposition based dynamic optimal power flow considering discrete and continuous decision variables," *IEEE Access*, vol. 8, pp. 194260–194268, 2020.

[7] H. Ambriz-Perez, E. Acha, and C. R. Fuerte-Esquivel, "Advanced SVC models for Newton-Raphson load flow and Newton optimal power flow studies," *IEEE Trans. Power Syst.*, vol. 15, no. 1, pp. 129–136, Feb. 2000.

[8] K. Zehar and S. Sayah, "Optimal power flow with environmental constraint using a fast successive linear programming algorithm: Application to the Algerian power system," *Energy Convers. Manag.*, vol. 49, no. 11, pp. 3362–3366, Nov. 2008.

[9] P. Fortenbacher and T. Demiray, "Linear/quadratic programming-based optimal power flow using linear power flow and absolute loss approximations," *Int. J. Electr. Power Energy Syst.*, vol. 107, pp. 680–689, May 2019.

[10] X. Yuan, B. Zhang, P. Wang, J. Liang, Y. Yuan, Y. Huang, and X. Lei, "Multi-objective optimal power flow based on improved strength Pareto evolutionary algorithm," *Energy*, vol. 122, pp. 70–82, Mar. 2017.

[11] T. Sousa, J. Soares, Z. A. Vale, H. Morais, and P. Faria, "Simulated annealing metaheuristic to solve the optimal power flow," in *Proc. IEEE Power Energy Soc. Gen. Meeting*, Detroit, MI, USA, Jul. 2011, pp. 1–8.

[12] M. A. Abido, "Optimal power flow using Tabu search algorithm," *Electr. Power Compon. Syst.*, vol. 30, no. 5, pp. 469–483, 2010.

[13] M. Ahmad, N. Javaid, I. A. Niaz, A. Almogren, and A. Radwan, "A bio-inspired heuristic algorithm for solving optimal power flow problem in hybrid power system," *IEEE Access*, vol. 9, pp. 159809–159826, 2021.

[14] P. P. Biswas, P. N. Suganthan, R. Mallipeddi, and G. A. J. Amaratunga, "Optimal power flow solutions using differential evolution algorithm integrated with effective constraint handling techniques," *Eng. Appl. Artif. Intell.*, vol. 68, pp. 81–100, Feb. 2018.

[15] A.-A. A. Mohamed, Y. S. Mohamed, A. A. M. El-Gaafary, and A. M. Hemeida, "Optimal power flow using moth swarm algorithm," *Electr. Power Syst. Res.*, vol. 142, pp. 190–206, Jan. 2017.

[16] K. Abaci and V. Yamacli, "Differential search algorithm for solving multi-objective optimal power flow problem," *Int. J. Electr. Power Energy Syst.*, vol. 79, pp. 1–10, Jul. 2016.

[17] S. Sivasubramani and K. S. Swarup, "Multi-objective harmony search algorithm for optimal power flow problem," *Int. J. Electr. Power Energy Syst.*, vol. 33, no. 3, pp. 745–752, Mar. 2011.

[18] S. Duman, "A modified moth swarm algorithm based on an arithmetic crossover for constrained optimization and optimal power flow problems," *IEEE Access*, vol. 6, pp. 45394–45416, 2018.

[19] M.-F. Leung, S.-C. Ng, C.-C. Cheung, and A. K. Lui, "A new algorithm based on PSO for multi-objective optimization," in *Proc. IEEE Congr. Evol. Comput. (CEC)*, Sendai, Japan, May 2015, pp. 3156–3162.

[20] M.-F. Leung, C. A. C. Coello, C.-C. Cheung, S.-C. Ng, and A. K.-F. Lui, "A hybrid leader selection strategy for many-objective particle swarm optimization," *IEEE Access*, vol. 8, pp. 189527–189545, 2020.

[21] M.-C. Yuen, S.-C. Ng, M.-F. Leung, and H. Che, "A Metaheuristic-based framework for index tracking with practical constraints," *Complex Intell. Syst.*, vol. 8, no. 6, pp. 4571–4586, Dec. 2022.

[22] W.-F. Gao, S.-Y. Liu, and L.-L. Huang, "A novel artificial bee colony algorithm based on modified search equation and orthogonal learning," *IEEE Trans. Cybern.*, vol. 43, no. 3, pp. 1011–1024, Jun. 2013.

[23] A. R. Bhowmik and A. K. Chakraborty, "Solution of optimal power flow using non dominated sorting multi objective opposition based gravitational search algorithm," *Int. J. Electr. Power Energy Syst.*, vol. 64, pp. 1237–1250, Jan. 2015.

[24] S. S. Reddy and C. S. Rathnam, "Optimal power flow using glow-worm swarm optimization," *Int. J. Elect. Power Energy Syst.*, vol. 80, pp. 128–139, Sep. 2016.

[25] H. Pulluri, R. Naresh, and V. Sharma, "A solution network based on stud krill herd algorithm for optimal power flow problems," *Soft Comput.*, vol. 22, no. 1, pp. 159–176, Jan. 2018.

[26] A. A. El-Fergany and H. M. Hasanien, "Tree-seed algorithm for solving optimal power flow problem in large-scale power systems incorporating validations and comparisons," *Appl. Soft Comput.*, vol. 64, pp. 307–316, Mar. 2018.

[27] A. Bhattacharya and P. K. Chattopadhyay, "Application of biogeography-based optimisation to solve different optimal power flow problems," *IET Gener., Transmiss. Distrib.*, vol. 5, no. 1, pp. 70–80, Jan. 2011.

[28] S. Duman, "Symbiotic organisms search algorithm for optimal power flow problem based on valve-point effect and prohibited zones," *Neural Comput. Appl.*, vol. 28, no. 11, pp. 3571–3585, Nov. 2017.

[29] E. Davoodi, E. Babaei, B. Mohammadi-Ivatloo, M. Shafie-Khah, and J. P. S. Catalao, "Multiobjective optimal power flow using a semidefinite programming-based model," *IEEE Syst. J.*, vol. 15, no. 1, pp. 158–169, Mar. 2021, doi: 10.1109/JSYST.2020.2971838.

[30] A. A. El-Fergany and H. M. Hasanien, "Salp swarm optimizer to solve optimal power flow comprising voltage stability analysis," *Neural Comput. Appl.*, vol. 32, no. 9, pp. 5267–5283, May 2020, doi: 10.1007/s00521-019-04029-8.

[31] M. A. Taher, S. Kamel, F. Jurado, and M. Ebeed, "Optimal power flow solution incorporating a simplified UPFC model using lightning attachment procedure optimization," *Int. Trans. Electr. Energy Syst.*, vol. 30, no. 1, Jan. 2020, Art. no. e12170, doi: 10.1002/2050-7038.12170.

[32] M. Z. Islam, N. I. A. Wahab, V. Veerasamy, H. Hizam, N. F. Mailah, J. M. Guerrero, and M. N. Mohd Nasir, "A Harris hawks optimization based single- and multi-objective optimal power flow considering environmental emission," *Sustainability*, vol. 12, no. 13, p. 5248, Jun. 2020, doi: 10.3390/su12135248.

[33] F. Daqaq, M. Ouassaid, and R. Ellaia, "A new meta-heuristic programming for multi-objective optimal power flow," *Electr. Eng.*, vol. 103, no. 2, pp. 1217–1237, Jan. 2021, doi: 10.1007/s00202-020-01173-6.

[34] M. Premkumar, P. Jangir, R. Sowmya, and R. M. Elavarasan, "Many-objective gradient-based optimizer to solve optimal power flow problems: Analysis and validations," *Eng. Appl. Artif. Intell.*, vol. 106, Nov. 2021, Art. no. 104479, doi: 10.1016/j.engappai.2021.104479.

[35] S. Khunkitti, A. Siritaratiwat, and S. Premrudeepreechacharn, "Multi-objective optimal power flow problems based on slime mould algorithm," *Sustainability*, vol. 13, no. 13, p. 7448, Jul. 2021, doi: 10.3390/su13137448.

[36] M. Z. Islam, M. L. Othman, N. I. A. Wahab, V. Veerasamy, S. R. Opu, A. Inbamani, and V. Annamalai, "Marine predators algorithm for solving single-objective optimal power flow," *PLoS ONE*, vol. 16, no. 8, Aug. 2021, Art. no. e0256050, doi: 10.1371/journal.pone.0256050.

[37] M. S. Kumari and S. Maheswarapu, "Enhanced genetic algorithm based computation technique for multi-objective optimal power flow solution," *Int. J. Elect. Power Energy Syst.*, vol. 32, no. 6, pp. 736–742, Jul. 2010.

[38] A. M. Shaheen, R. A. El-Sehiemy, and S. M. Farrag, "Solving multi-objective optimal power flow problem via forced initialised differential evolution algorithm," *IET Gener., Transmiss. Distrib.*, vol. 10, no. 7, pp. 1634–1647, May 2016.

[39] V. Raviprabakaran and R. C. Subramanian, "Enhanced ant colony optimization to solve the optimal power flow with ecological emission," *Int. J. Syst. Assurance Eng. Manag.*, vol. 9, no. 1, pp. 58–65, Feb. 2018.

[40] W. Bai, I. Eke, and K. Y. Lee, "An improved artificial bee colony optimization algorithm based on orthogonal learning for optimal power flow problem," *Control Eng. Pract.*, vol. 61, pp. 163–172, Apr. 2017.

[41] H. R. E. H. Bouchekara, A. E. Chaib, M. A. Abido, and R. A. El-Sehiemy, "Optimal power flow using an improved colliding bodies optimization algorithm," *Appl. Soft Comput.*, vol. 42, pp. 119–131, May 2016.

[42] N. Daryani, M. T. Hagh, and S. Teimourzadeh, "Adaptive group search optimization algorithm for multi-objective optimal power flow problem," *Appl. Soft Comput.*, vol. 38, pp. 1012–1024, Jan. 2016.

[43] H. R. E. H. Bouchekara, A. E. Chaib, and M. A. Abido, "Optimal power flow using GA with a new multi-parent crossover considering: Prohibited zones, valve-point effect, multi-fuels and emission," *Electr. Eng.*, vol. 100, no. 1, pp. 151–165, Mar. 2018.

[44] S. S. Reddy and P. R. Bijwe, "Efficiency improvements in meta-heuristic algorithms to solve the optimal power flow problem," *Int. J. Elect. Power Energy Syst.*, vol. 82, pp. 288–302, Nov. 2016.

[45] A. F. Attia, R. A. El Sehiemy, and H. M. Hasanien, "Optimal power flow solution in power systems using a novel sine-cosine algorithm," *Int. J. Electr. Power Energy Syst.*, vol. 99, pp. 331–343, Jun. 2018.

[46] Y. Muhammad, R. Khan, M. A. Z. Raja, F. Ullah, N. I. Chaudhary, and Y. He, "Design of fractional swarm intelligent computing with entropy evolution for optimal power flow problems," *IEEE Access*, vol. 8, pp. 111401–111419, 2020.

[47] W. Ongsakul and T. Tantimaporn, "Optimal power flow by improved evolutionary programming," *Electric Power Compon. Syst.*, vol. 34, no. 1, pp. 79–95, Jan. 2006.

[48] T. Niknam, M. R. Narimani, M. Jabbari, and A. R. Malekpour, "A modified shuffle frog leaping algorithm for multi-objective optimal power flow," *Energy*, vol. 36, no. 11, pp. 6420–6432, Nov. 2011.

[49] T. Niknam, M. R. Narimani, J. Aghaei, and R. Azizipanah-Abarghooee, "Improved particle swarm optimisation for multi-objective optimal power flow considering the cost, loss, emission and voltage stability index," *IET Gener., Transmiss. Distrib.*, vol. 6, no. 6, pp. 515–527, Jun. 2012.

[50] N. Sinsuphan, U. Leeton, and T. Kulworawanichpong, "Optimal power flow solution using improved harmony search method," *Appl. Soft Comput.*, vol. 13, no. 5, pp. 2364–2374, May 2013.

[51] R. Arul, G. Ravi, and S. Velusami, "Solving optimal power flow problems using chaotic self-adaptive differential harmony search algorithm," *Electric Power Compon. Syst.*, vol. 41, no. 8, pp. 782–805, May 2013.

[52] K. Pandiarajan and C. K. Babulal, "Fuzzy harmony search algorithm based optimal power flow for power system security enhancement," *Int. J. Electr. Power Energy Syst.*, vol. 78, pp. 72–79, Jun. 2016.

[53] P. P. Biswas, P. N. Suganthan, R. Mallipeddi, and G. A. J. Amaratunga, "Multi-objective optimal power flow solutions using a constraint handling technique of evolutionary algorithms," *Soft Comput.*, vol. 24, no. 4, pp. 2999–3023, Feb. 2020.

[54] S. S. Reddy, P. R. Bijwe, and A. R. Abhyankar, "Faster evolutionary algorithm based optimal power flow using incremental variables," *Int. J. Elec. Power.*, vol. 54, pp. 198–210, Sep. 2014.

[55] J. C. Bansal and P. Farswan, "A novel disruption in biogeography-based optimization with application to optimal power flow problem," *Int. J. Speech Technol.*, vol. 46, no. 3, pp. 590–615, Apr. 2017.

[56] M. Abdo, S. Kamel, M. Ebeed, J. Yu, and F. Jurado, "Solving non-smooth optimal power flow problems using a developed grey wolf optimizer," *Energies*, vol. 11, no. 7, p. 1692, Jun. 2018.

[57] G. Chen, Z. Lu, and Z. Zhang, "Improved krill herd algorithm with novel constraint handling method for solving optimal power flow problems," *Energies*, vol. 11, no. 1, p. 76, Jan. 2018.

[58] H. Pulluri, R. Naresh, and V. Sharma, "An enhanced self-adaptive differential evolution based solution methodology for multiobjective optimal power flow," *Appl. Soft Comput.*, vol. 54, pp. 229–245, May 2017.

[59] A. M. Shaheen, S. M. Farrag, and R. A. El-Sehiemy, "MOPF solution methodology," *IET Gener., Transmiss. Distrib.*, vol. 11, no. 2, pp. 570–581, Jan. 2017.

[60] X. Zhou, A. Su, A. Liu, W. Cui, and W. Liu, "Cooperative approach to artificial bee colony algorithm for optimal power flow," *Cluster Comput.*, vol. 22, pp. 8059–8067, Jul. 2019.

[61] G. Chen, J. Qian, Z. Zhang, and S. Li, "Application of modified pigeon-inspired optimization algorithm and constraint-objective sorting rule on multi-objective optimal power flow problem," *Appl. Soft Comput.*, vol. 92, Jul. 2020, Art. no. 106321.

[62] T. T. Nguyen, "A high performance social spider optimization algorithm for optimal power flow solution with single objective optimization," *Energy*, vol. 171, pp. 218–240, Mar. 2019.

[63] M. A. Taher, S. Kamel, F. Jurado, and M. Ebeed, "An improved moth-flame optimization algorithm for solving optimal power flow problem," *Int. Trans. Electr. Energy Syst.*, vol. 29, no. 3, p. e2743, Mar. 2019.

[64] M. A. Taher, S. Kamel, F. Jurado, and M. Ebeed, "Modified grasshopper optimization framework for optimal power flow solution," *Elect. Eng.*, vol. 101, no. 1, pp. 121–148, Apr. 2019.

[65] H. Bouchekara, "Solution of the optimal power flow problem considering security constraints using an improved chaotic electromagnetic field optimization algorithm," *Neural Comput. Appl.*, vol. 32, no. 7, pp. 2683–2703, Apr. 2020.

[66] H. Buch and I. N. Trivedi, "An efficient adaptive moth flame optimization algorithm for solving large-scale optimal power flow problem with POZ, multifuel and valve-point loading effect," *Iranian J. Sci. Technol., Trans. Electr. Eng.*, vol. 43, no. 4, pp. 1031–1051, Dec. 2019.

[67] X.-B. Meng, X. Z. Gao, L. Lu, Y. Liu, and H. Zhang, "A new bio-inspired optimisation algorithm: Bird swarm algorithm," *J. Exp. Theor. Artif. Intell.*, vol. 28, pp. 673–687, Jun. 2015.

[68] X. Wang, Y. Deng, and H. Duan, "Edge-based target detection for unmanned aerial vehicles using competitive bird swarm algorithm," *Aerosp. Sci. Technol.*, vol. 78, pp. 708–720, Jul. 2018.

[69] Z.-H. Zhan, J. Zhang, Y. Li, and Y.-H. Shi, "Orthogonal learning particle swarm optimization," *IEEE Trans. Evol. Comput.*, vol. 15, no. 6, pp. 832–847, Dec. 2011.

[70] Y.-W. Leung and Y. Wang, "An orthogonal genetic algorithm with quantization for global numerical optimization," *IEEE Trans. Evol. Comput.*, vol. 5, no. 1, pp. 41–53, Feb. 2001.

MANZOOR AHMAD received the M.Sc. degree in computer science from Quaid-i-Azam University, Islamabad, Pakistan, the M.S. degree in computer science from Mälardalens Högskola Eskilstuna Västerås, Sweden, and the Ph.D. degree in computer science from COMSATS University Islamabad, Islamabad Campus, Pakistan, under the supervision of Dr. Iftikhar Azim Niaz and co-supervision of Dr. Nadeem Javaid. He has been with COMSATS University Islamabad, since 2003. His research interests include artificial intelligence and optimal power flow.
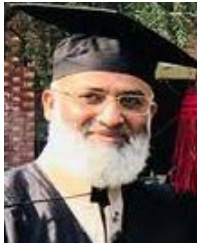
NADEEM JAVAID (Senior Member, IEEE) received the bachelor's degree in computer science from Gomal University, Dera Ismail Khan, Pakistan, in 1995, the master's degree in electronics from Quaid-i-Azam University, Islamabad, Pakistan, in 1999, and the Ph.D. degree from the University of Paris-Est, France, in 2010. He is currently a tenured Professor and the Founding Director of the Communications Over Sensors (ComSens) Research Laboratory, Department of Computer Science, COMSATS University Islamabad, Islamabad Campus. He has supervised 158 master's and 30 Ph.D. theses. He has authored more than 900 papers in technical journals and international conferences. His research interests include energy optimization in smart/microgrids and wireless sensor networks using data analytics and blockchain. He was a recipient of the Best University Teacher Award (BUTA 2016) from the Higher Education Commission (HEC), Pakistan, in 2016, and the Research Productivity Award (RPA 2017) from the Pakistan Council for Science and Technology (PCST), in 2017.

IJAZ AHMED received the M.Sc. degree in computer sciences from the Queen Mary University of London and the Ph.D. degree in computer sciences from the University of Madeira, Portugal. He is currently an Assistant Professor with the University of Technology and Applied Sciences, Ibri, Oman. Previously, he has worked as a Faculty Member with COMSATS University Islamabad, Pakistan. Besides this, he was also a Senior Research Fellow with the Internet of Things and Security Center, Greenwich University, London, and a Senior Scientist with UNIST, South Korea. He has published numerous research papers in conferences and journals of international repute.

IFTIKHAR AZIM NIAZ (Senior Member, IEEE) has been a Ph.D. Supervisor of the Higher Education Commission (HEC), since 2007. Because of his professional experience, expertise, and social and communication skills, he has been on the Expert Panel of the PEC Accreditation Team, since 2009. He is currently a Professional Engineer, an Assistant Professor, and the Ph.D. Coordinator with the Department of Computer Science. He has been coordinating with different government and private sectors and organizations, improving the academic standard of students. His research interests include wireless sensor networks, energy optimization in smart grids, and software engineering. He is a member of various national and international professional bodies and clubs which is one of the necessary conditions for managing projects.

MUHAMMAD ADNAN HASHMI received the master's degree in artificial intelligence from University Rene Descartes (currently the University of Paris) and the Ph.D. degree in artificial intelligence from Pierre and Marie Curie University (currently Sorbonne University). He has been with the Higher Colleges of Technology, United Arab Emirates, since 2019. He has 15 years of teaching and research experience. His research interests include the development of agent-oriented programming languages and multi-agent coordination mechanisms.

● ● ●